

NOLC REPORT 694

31 OCTOBER 1966

NOLC REPORT 694

AD 646629

**SELECTION OF A VLF RECEIVING ANTENNA
FOR THE BOLIVIAN SOLAR ECLIPSE SITE**

V. E. HILDEBRAND

RESEARCH DEPARTMENT

**DDC
REFORMED
FEB 14 1967
RECEIVED
B**

**Distribution of this document
is unlimited.**



**NAVAL ORDNANCE LABORATORY CORONA
CORONA, CALIFORNIA**

ARCHIVE COPY

NAVAL ORDNANCE LABORATORY CORONA

E. B. JARMAN, CAPT., USN
Commanding Officer

F. S. ATCHISON, Ph. D.
Technical Director

ABSTRACT

Properties of the ionosphere D region under conditions of a solar total eclipse are to be measured utilizing a VLF receiving system in Bolivia. The signals will be transmitted from southeast Brazil along the path of totality for the 12 November 1966 solar eclipse.

This report describes the study conducted for the selection of a VLF receiving antenna which will provide maximum discrimination against atmospheric noise in the 9- to 31-kc band. The antenna selected was a two-loop superdirective antenna with the loop elements rotated 25° from the antenna axis. The report describes the criteria utilized in selecting the antenna, discusses other possible choices, and evaluates the performance of the antenna in the light of various component tolerances.

ADDITIONAL TO

WHITE SECTION

WHITE SECTION

ADVANCED

RELATION

SECTION/AVAILABILITY CODES

DIST.	AVAIL.	SP. SPECIAL
/		

FOREWORD

The antenna study described in this report is a part of the broad program of research in the field of VLF radio signals which has been in progress in the Electronics Division at the Naval Ordnance Laboratory Corona over a period of several years.

The work covered in this report was undertaken in preparation for the establishment of a VLF receiving site in Bolivia. This project was sponsored by the Defense Atomic Support Agency, REAL, under MIPER 555-67.

C. J. HUMPHREYS
Head, Research Department

CONTENTS

	<u>Page</u>
INTRODUCTION	1
SIGNAL ENVIRONMENT	1
EVALUATION OF ANTENNA TYPES	5
Loop Antenna	5
Two-Loop Superdirective Antenna	5
Superdirective Antenna Patterns	8
ANTENNA PERFORMANCE ANALYSIS	11
Procedures	11
Loop Separation	13
Loop Misalignment	17
Performance Characteristics	17
PRACTICAL CONSIDERATIONS	30

INTRODUCTION

Personnel of the Naval Ordnance Laboratory, Corona are planning to investigate the properties of the ionosphere D region as they are affected by the solar total eclipse of 12 November 1966. Data will be acquired by measuring the variation of VLF radio signals, reflected at the D region, and propagated along the eclipse path of totality. To accomplish these measurements a VLF receiving system will be located at Tarija, Bolivia ($21^{\circ} 30' \text{ S.}$, $64^{\circ} 40' \text{ W.}$), and a VLF transmitting system will be located near Pinheiro Machado, Brazil ($31^{\circ} 40' \text{ S.}$, $53^{\circ} 32' \text{ W.}$). The transmitting and receiving sites are beneath the path of totality for the D region of the ionosphere. The propagation path is approximately 1,500 km in length and lies in a direction of 313° true.

The transmission will consist of short pulses of approximately 320 μsec duration with 8 frequencies between 9 and 31 kc transmitted sequentially. The frequencies will be scrambled in order to maintain a maximum frequency separation between adjacent transmissions, each frequency being radiated 10 percent of the time. The transmission will be at very low power; therefore, it will be necessary to achieve the maximum sensitivity in the receiving equipment. As is typical for VLF the receiving sensitivity limitation is the atmospheric noise level produced by the thunderstorm activity within a wide geographical area, in this case including all of South America, Central America, the Caribbean area, and possibly Africa.

The objective of this investigation was to select a VLF receiving antenna which would be usable over the 9- to 31-kc band and provide the maximum discrimination against atmospheric noise at the receiving location. The antenna selected was a two-loop superdirective antenna in which the loop elements were rotated 25° with respect to the antenna axis. This report describes the criteria utilized to arrive at the selection of this antenna, discusses other possible choices, justifies the selection of the particular antenna, and evaluates the performance of this antenna in the light of various component tolerances.

SIGNAL ENVIRONMENT

The transmissions will be received from a bearing of 133° true. The incident field strength will be between 10 and 30 $\mu\text{v/m}$, depending

upon frequency, during daytime propagation conditions along the path and between 10 and 60 $\mu\text{v}/\text{m}$ during all nighttime conditions along the path. In contrast the atmospheric noise produced by thunderstorm lightning activity will have signal levels on the order of volts per meter. The centers of thunderstorm activity in close proximity to the receiving site are illustrated in Figure 1, which also illustrates the path of totality for the eclipse and the VLF transmission path. The most intense thunderstorm activity in terms of thunderstorm days for November is centered at 15° S. , 60° W. at approximately 90° from the transmission path at the receiver location. The expected thunderstorm activity is indicated by countour lines beginning at 25 thunderstorm days for the month at the above coordinates and decreasing in increments of 5 to a value of 10 thunderstorm days. It will be noted that the region of low activity is distributed over a wide geographical area, generally north-east of the path of the eclipse. In Figure 2 it will be noted that all significant thunderstorm activity which produces interfering atmospheric noise lies north of the eclipse path of totality, and that the area south of the path is generally devoid of activity.

For analysis purposes the thunderstorm activity which produces interfering noise has been divided into the following zones, which are based on the thunderstorm-day contours shown in Figure 1.

Zone I: this zone is the region within the 20-day contour; it is a 15° sector centered at approximately 45° true from the receiving site at a range of 700 km with a depth of 50 km.

Zone II: this zone is the region bounded by the 15-day contour; it is a 40° sector, also at 45° true from the receiving site and at a range of 700 km, but with a depth of 200 km.

Zone III: this zone is the region within the 15-day contour north-east of Zone II; it is a 60° sector, again approximately 45° true from the receiving site, but at a range of 1,400 km with a depth of approximately 300 km.

Zone IV: this zone encompasses the remaining significant activity and is specified as a 140° sector centered at 10° true from the receiving site with a depth ranging from approximately 200 km to infinity. This sector includes the atmospheric noise centers in Panama, the Caribbean area, the Amazon River basin, and Africa, all of which are intense activity centers but lie a long distance from the receiving site.

The VLF antenna will be utilized to simultaneously receive transmissions over the frequency band from 9 to 31 kc; thus, the antenna

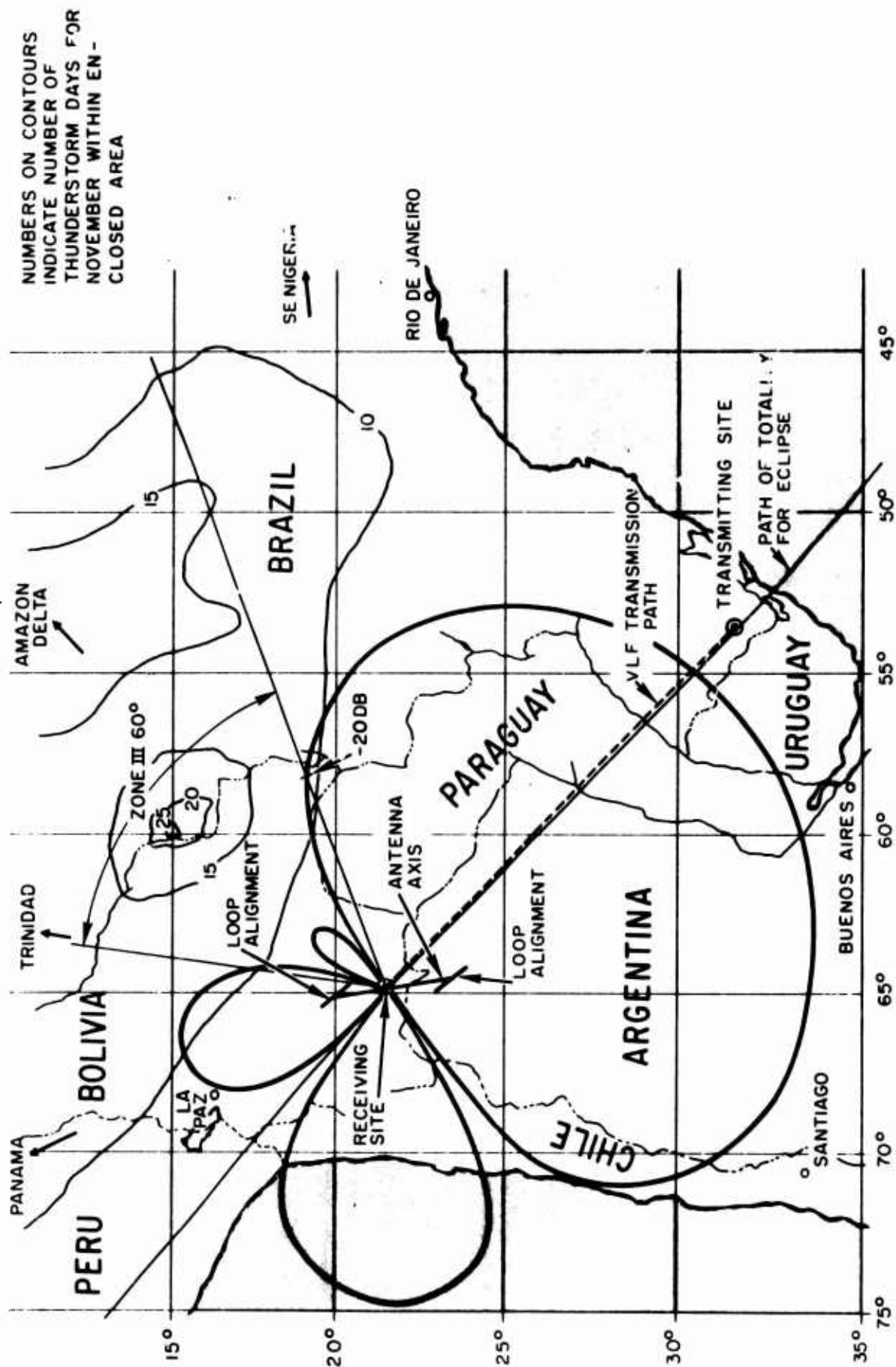


FIGURE 1. Solar Eclipse Path of Totality and Location of VLF Transmitting and Receiving Sites, Showing Receiving-Antenna Pattern and Atmospheric Noise Areas

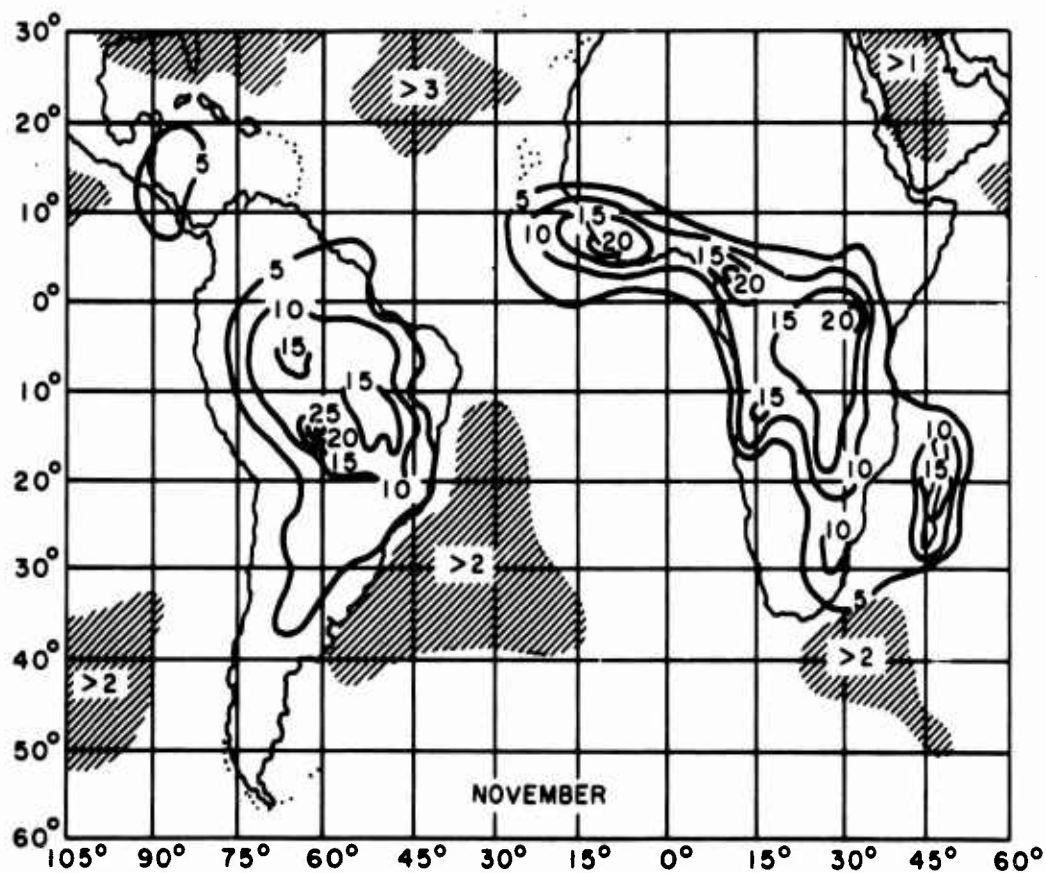
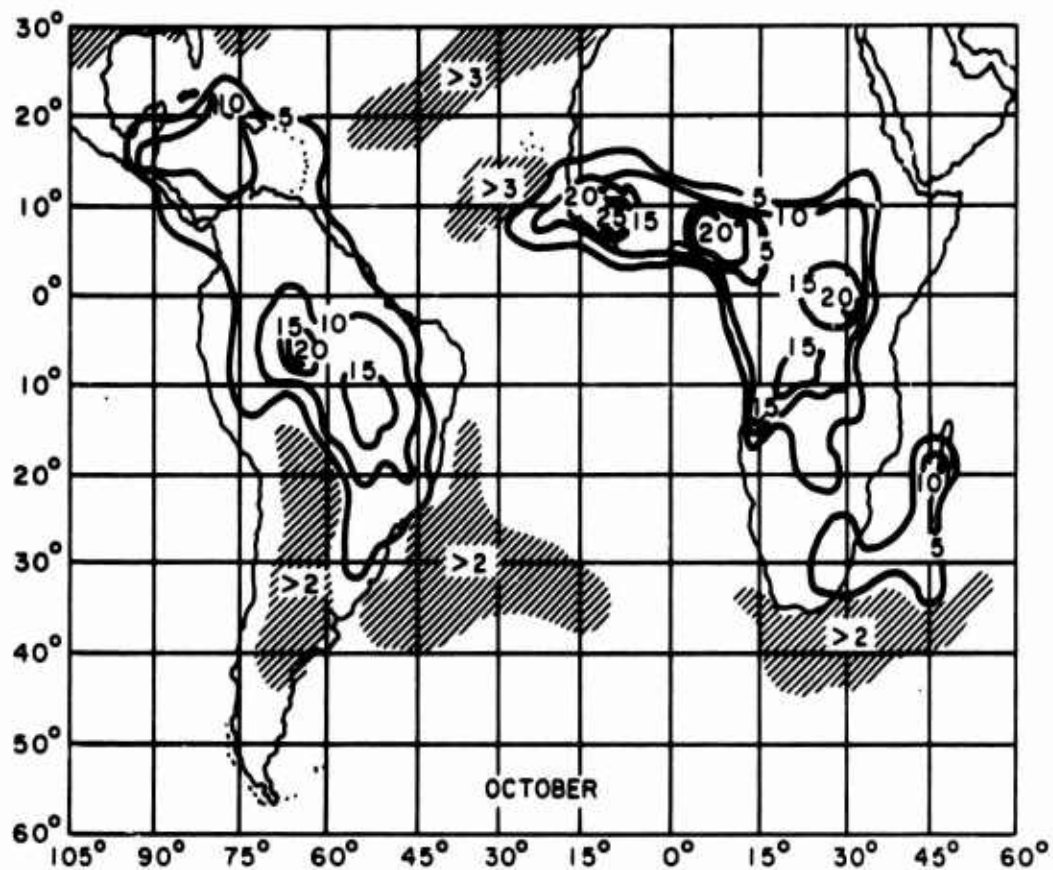


FIGURE 2. Thunderstorm Days per Month

must be broadband. The atmospheric-noise spectral characteristics expected within this band are illustrated in Figure 3. (The reader is reminded that the November eclipse will occur during the summer season in Bolivia.)

EVALUATION OF ANTENNA TYPES

The initial task of this investigation was to evaluate the noise-discrimination potential for various idealized antenna patterns and to select the best antenna configuration. The final task was then to evaluate the expected performance of the selected antenna as affected by the performance tolerances of the components.

LOOP ANTENNA

The loop antenna is most frequently used for VLF reception because of its compactness, reliability, and consistency of performance. However, this antenna provides little discrimination against atmospheric noise because of its figure-8 antenna pattern and 90° half-power beamwidth. The pattern null, although quite deep, is also very narrow; see the pattern in Figure 4 plotted linear in db. If the loop antenna is oriented to provide the greatest discrimination against noise in Zone I, the VLF transmissions will be received at 0° on the pattern. It will be noted in Figure 4 that the edges of Zone I are only 17 db down from maximum; thus, only about 20-db discrimination against atmospheric noise is achieved (10-to-1 discrimination in voltage). Correspondingly the boundary lines of Zone II are at -9 db and the edges of Zone III are only 6 db down. Obviously, this antenna does not provide as much discrimination against atmospheric noise as desired. However, it is a commonly used antenna, and therefore provides a good reference for comparison with other antennas.

TWO-LOOP SUPERDIRECTIVE ANTENNA

A class of receiving antennas, which makes use of the principle of superdirectivity, has been under investigation at NOLC for some time.^{1,2} These antennas are electrically short, element spacing being typically 0.1λ . They are relatively frequency independent, maintaining good pattern characteristics over the 9- to 31-kc band, and have a high main-

¹NOLC Report 562, The Two-Loop Superdirective End-Fire Antenna, by E. W. Seeley. 1 April 1962.

²NOLC Report 624, More About Superdirective Antennas for LF and VLF, by V. E. Hildebrand. 28 May 1965.

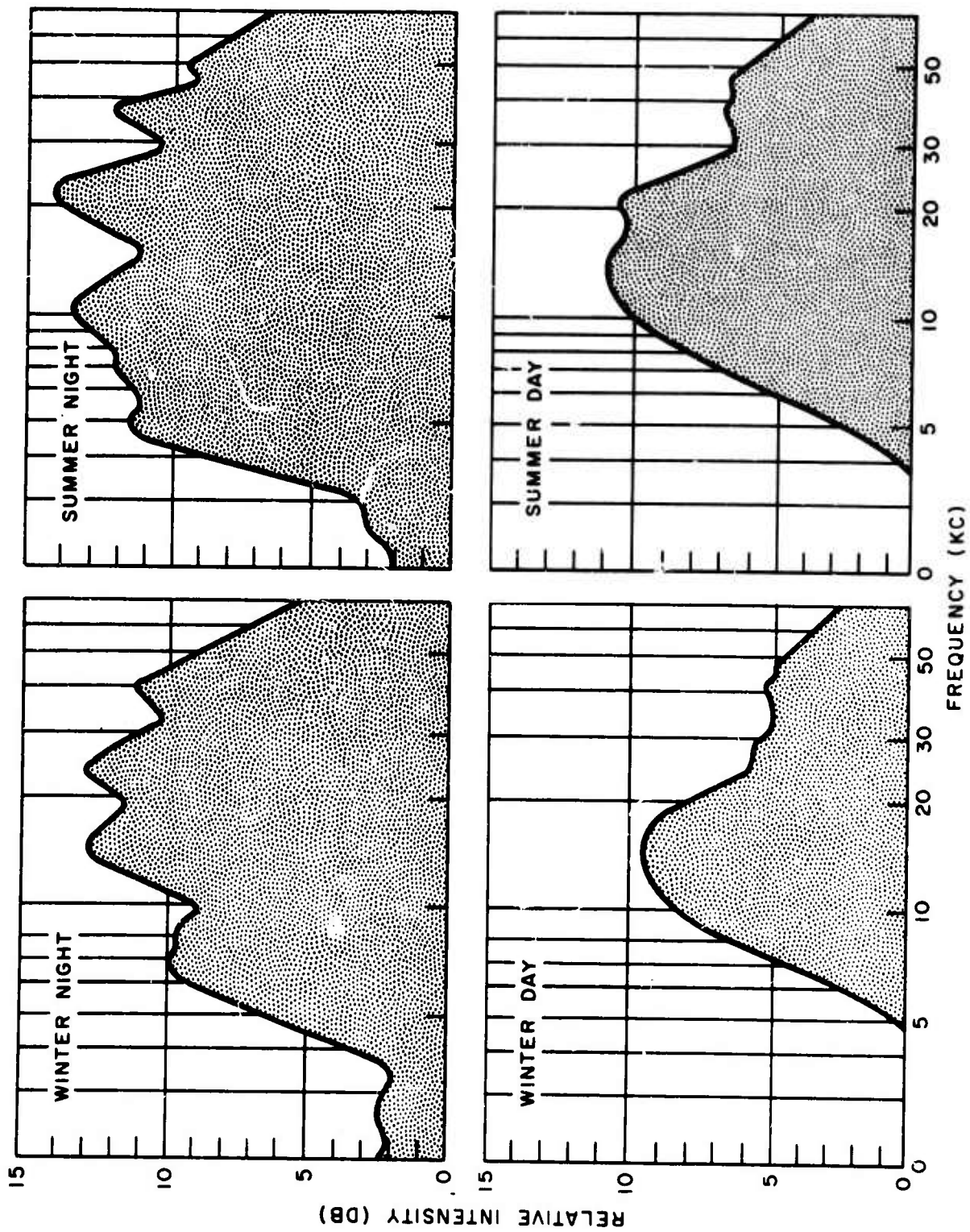


FIGURE 3. Atmospheric-Noise Spectral Characteristics

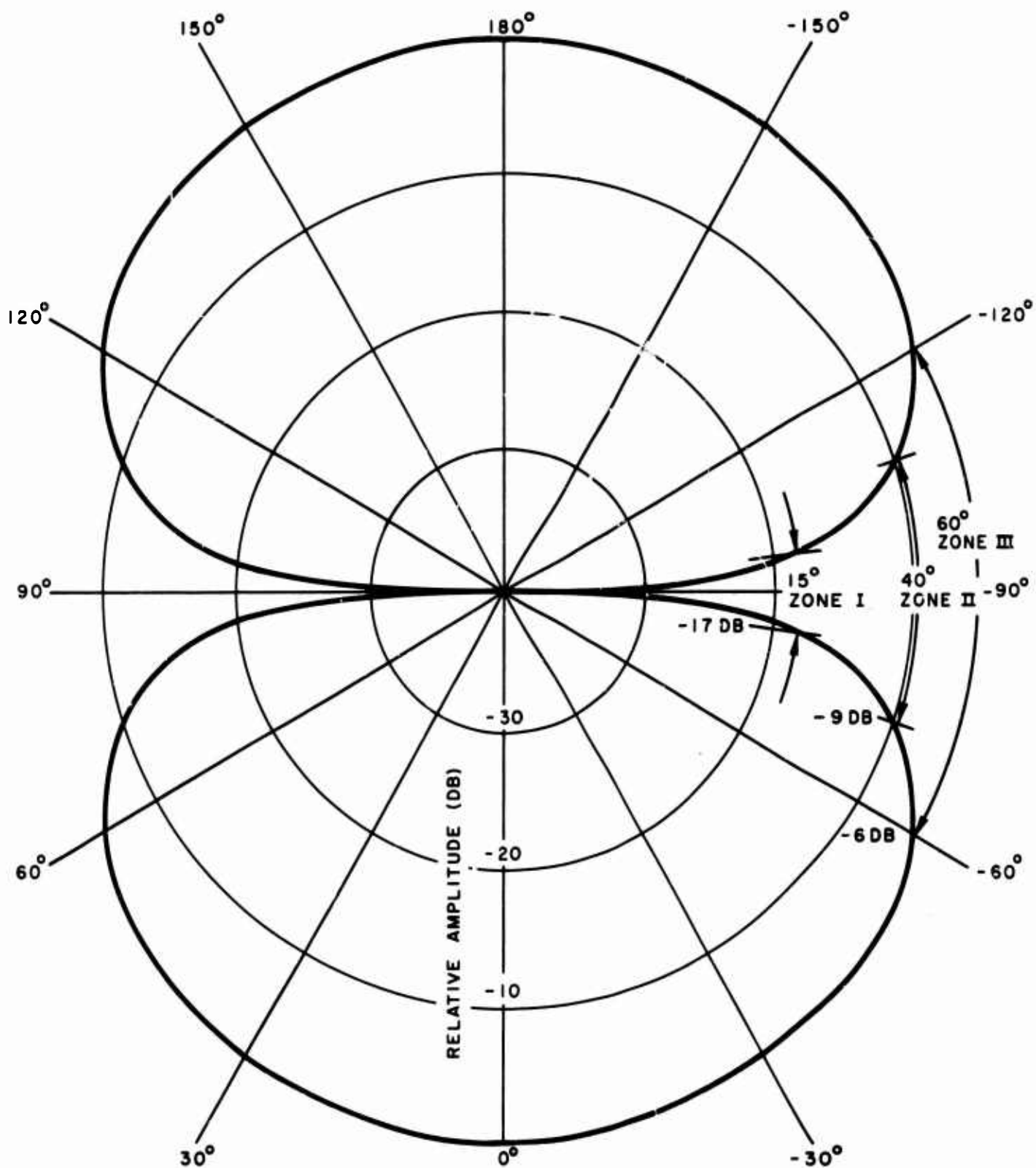


FIGURE 4. Loop-Antenna Pattern, Showing Relationship of Null to Noise Zones

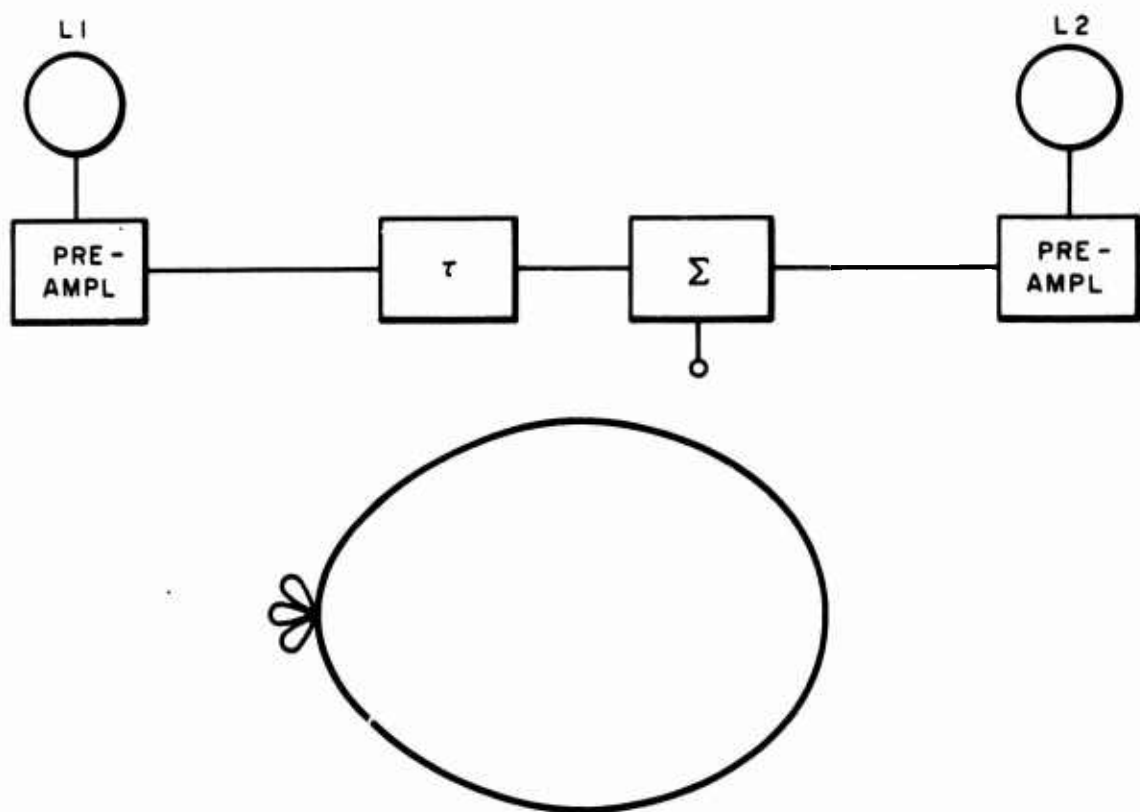
lobe-to-minor-lobe ratio. The main beam is relatively wide, being approximately 70° ; thus, the antenna value is primarily that of discrimination against interference propagated from the rear quadrants. A block diagram and pattern of a two-loop, superdirective antenna is presented in Figure 5 along with the pattern equation.

The two-loop antenna has found the widest application of the various superdirective configurations primarily because of its relative simplicity and its shorter length. Considerable flexibility is available in the choice of parameters for the superdirective antenna. In the past, however, application has been generally restricted to the utilization of a symmetrical pattern, varying only the null positions between minor lobes and therefore the relative amplitude of the minor lobes. Figure 6 illustrates the pattern of a two-loop superdirective antenna plotted linearly in db. This pattern illustrates two configurations of minor lobes: the first has two minor lobes with a null at 180° ; the second has three approximately equal-amplitude minor lobes with nulls at $\pm 146^\circ$. In practice this null can be placed at any angle between $\pm 90^\circ$ and 180° , with corresponding variations in the relative amplitudes of the minor lobes. For null angles of less than $\pm 146^\circ$, the center backlobe is largest. For null angles greater than $\pm 146^\circ$, the side lobes are larger than the backlobe. The optimum orientation for this antenna at the Bolivian receiving site would be for the antenna axis (0° on pattern) to be directed 3° clockwise from the azimuth of the received signal as indicated in Figure 6.

A comparison of Figures 4 and 6 shows that the two-loop antenna offers a significant improvement in noise discrimination. The sensitivity to Zone I is down 25 db as compared with about 17 db for the simple loop; the sensitivity to Zone II is down about 18 to 20 db as compared with 9 db; and the eastern edge of Zone III is at 8 db as compared with 6 db. Some additional improvement in discrimination could possibly be achieved by rotating the pattern null farther clockwise; however, the backlobe would increase in value thereby raising the sensitivity to atmospheric noise generated in the general area towards Central America. The possibilities for further improvements of this nature are very difficult to assess in the planning stages. If improvements are achievable, this can be best assessed and obtained in the field, since the null positions are adjustable with equipment settings. Further improvements in antenna performance can be achieved by skewing the antenna pattern as will be illustrated in the next section.

SUPERDIRECTIVE ANTENNA PATTERNS

It had been known for some time that the receiving pattern of the superdirective antenna could be skewed by rotating the plane of the loops



$$E_{\phi} = 2 \cos \phi \sin \left[\left(\frac{\pi D}{\lambda} \right) \cos \phi + \left(\frac{\theta}{2} \right) \right]$$

WHERE

E_{ϕ} = RELATIVE AMPLITUDE OF VOLTAGE RECEIVED FROM A DIRECTION ϕ

D = DISTANCE BETWEEN LOOPS

λ = WAVELENGTH

θ = PULSE DELAY OR ADVANCE BETWEEN LOOPS (DETERMINED BY τ)

FIGURE 5. Two-Loop Superdirective Antenna, Block Diagram and Pattern Equation

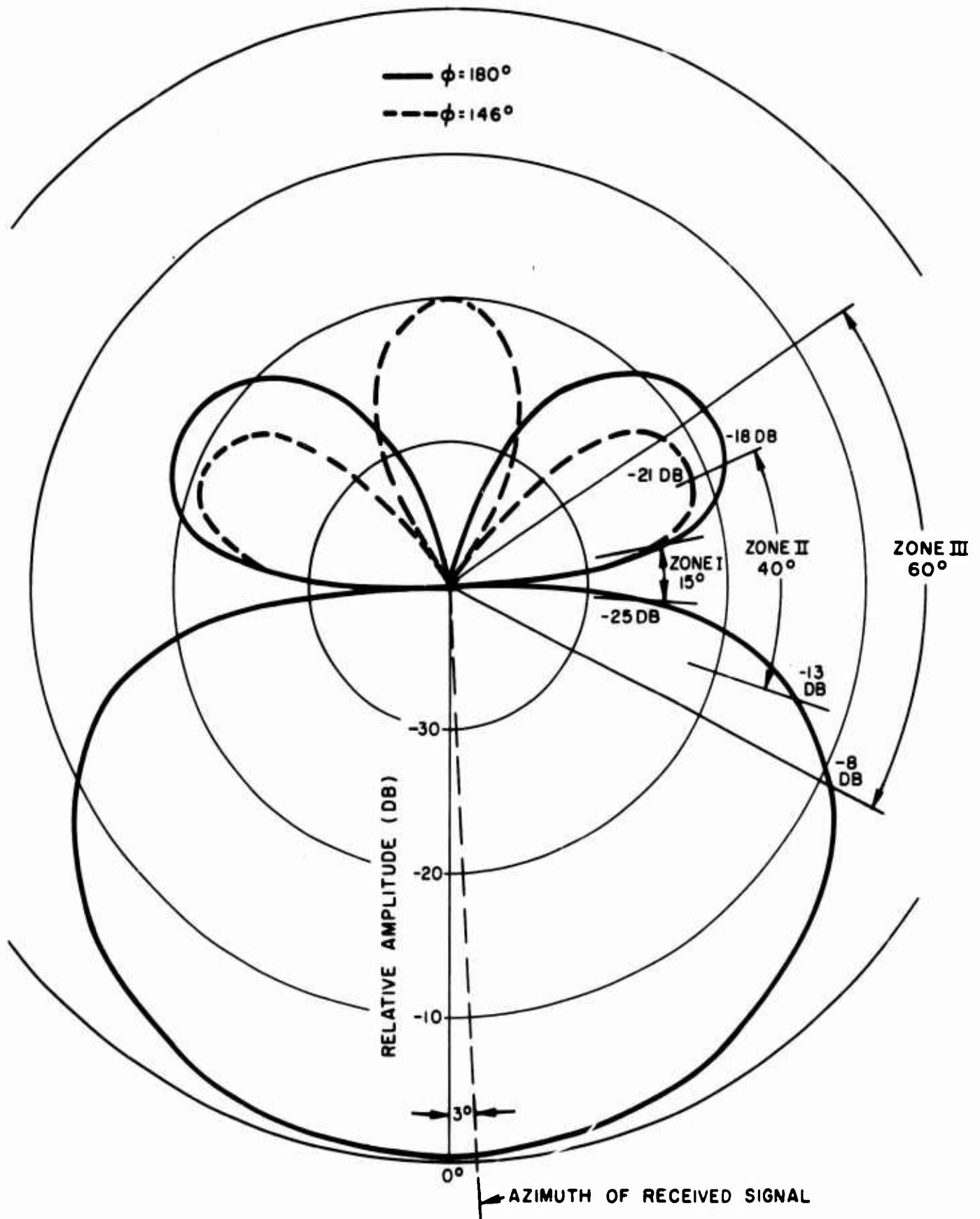


FIGURE 6. Two-Loop Superdirective-Antenna Pattern

with respect to the axis of the antenna. This rotation causes both the main lobe and the minor lobes to be distorted so that they are no longer symmetrical about the antenna axis. This rotation causes the main lobe to become broader in the direction of rotation of the loops. Continuing around the pattern in the direction of loop rotation, the first minor lobe becomes considerably smaller with the opposite minor lobe generally getting much larger. The center or back minor lobe is not greatly affected. An example of such a pattern is shown in Figure 7, which is the pattern for a two-loop array with a 1.1-mi spacing between elements and the plane of the loops rotated 25° from the antenna axis. The axis of the antenna, which is the line of sight between the loop elements, is indicated by 0° on this pattern. The null angle was set at 146° . In comparing this pattern with that of Figure 6, it appeared that this antenna configuration would be advantageous if the atmospheric noise came from a sector on one side and to the rear of the antenna. However, it was realized that the performance tolerances necessary to maintain this pattern are significantly more stringent than for a symmetrical pattern. Therefore, a very careful evaluation of the potential for maintaining the antenna-pattern configuration was needed.

For the conditions existing at the Bolivian receiving site, an antenna orientation of 174° was chosen, thus placing the axis of the antenna 40° south of the signal bearing (see Figure 1). In this position most of the main lobe and the large side lobe are oriented in a generally southern direction where very little thunderstorm activity occurs. With this pattern the sensitivity to noise originating in Zones I and II is down 30 db; in Zone III it is down 20 db, as shown in Figure 7. Another advantage of this pattern configuration is that the backlobe of the pattern is reasonably low and thus the sensitivity is minimized to atmospheric noise originating along the north coast of South America and in Central America.

Of the antenna configurations considered, the one with the pattern shown in Figure 7 is the best for the requirements of the Bolivian receiving site. If this pattern can be closely approximated in practice marked improvements in received signal-to-noise ratio (S/N) can be obtained. The question then becomes one of determining the component tolerance requirements for an antenna that will have acceptable performance.

ANTENNA PERFORMANCE ANALYSIS

PROCEDURES

Referring to the block diagram presented in Figure 5, those antenna-component tolerances which need to be evaluated include the mechanical

FREQUENCY = 20 KC
 1.1-MI SPACING
 BETWEEN ELEMENTS
 $\phi = 146^\circ$

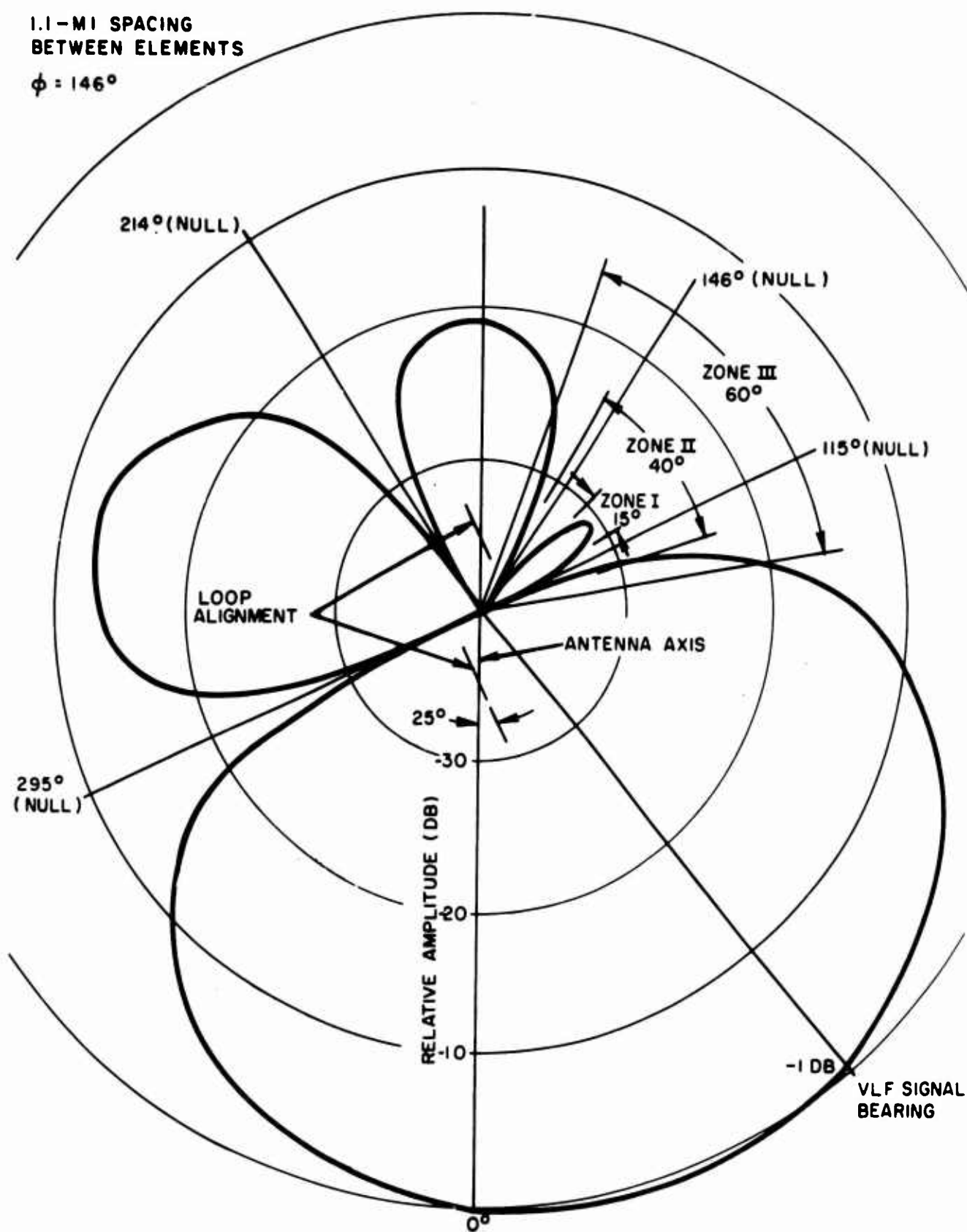


FIGURE 7. Pattern of Two-Loop Superdirective Antenna
 With Loops Rotated 25° From Antenna Axis

tolerances of the loops; the loop physical alignment; the preamplifier gain and phase stability; phase shift within the preamplifiers; transmission-line bandpass characteristics; transmission line attenuation and phase stability; standing-wave effects produced by small mismatches to the transmission line; properties of the matching transformers from the loop to the preamplifier, from the preamplifier to the transmission line, and from the transmission line to the summation network; and the properties of the lumped constant delay line and summation panel. Detailed information on the performance of all components was not available; therefore, this analysis was undertaken on the basis that a range of variables between ideal and expected worst-case conditions would be examined. The information acquired was then to be used to establish design criteria for the components.

A computer program error analysis of superdirective antennas has been developed.³ This program has great flexibility; thus, it is possible to examine many of the interrelationships of concern in this study. Previous error-analysis studies have demonstrated that, in general, the tolerances are tightest at the lowest frequency under consideration. Also, the atmospheric-noise power is greatest at the low end of the band, 10 kc (see Figure 3). Because of this, most of the analysis was conducted at 10 kc with occasional checks made at 20 kc and 30 kc.

LOOP SEPARATION

Selection of the antenna length (loop separation) is based on a combination of practical considerations and performance criteria. By the nature of the frequencies involved the distance is large (approximately 1 mi). The advantages of making an antenna shorter are (1) smaller land area required, (2) shorter transmission lines, (3) greater main-lobe-to-minor-lobe ratios, and (4) narrower beamwidth; the general disadvantage is that closer tolerances are required for achievement of a specified performance. Analysis has shown that there is an optimum loop separation for the 20-kc bandwidth (10 to 30 kc) with a given set of tolerance boundary values. As an example, the pattern dispersion was examined at three frequencies and three separation distances (D) for the condition where the misalignment of the plane of the loops ($\Delta\alpha$) was 2° . These patterns are shown in Figures 8, 9, and 10.⁴ Comparisons

³NOLC Report 686, Design and Error Analysis of VLF Superdirective Antenna Arrays, by J. N. Martin and J. R. Hill. 21 October 1966.

⁴The patterns presented in this error analysis are envelope patterns representing the worst-case condition within the tolerance boundaries at each angle of the pattern.

$\Delta \alpha = 2^\circ$
 RENULLED AT 146°
 --- D = 0.7 MI
 — D = 1.1 MI
 --- D = 1.5 MI

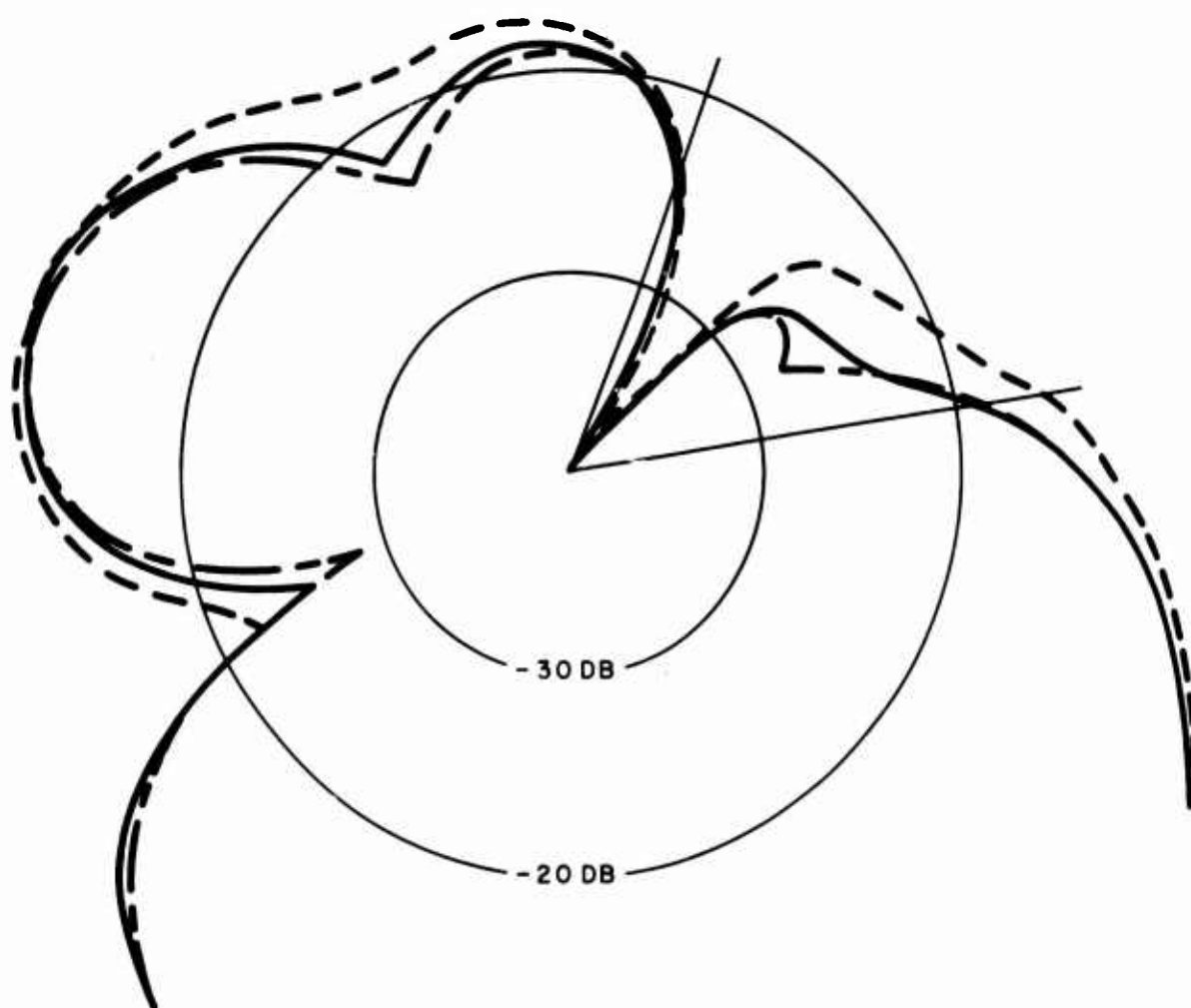


FIGURE 8. Envelope Patterns for Various Loop-Separation Distances at 10 kc

$\Delta\alpha = 2^\circ$

RENULLED AT 146°

----- D=0.7 MI

----- D=1.1 MI

———— D=1.5 MI

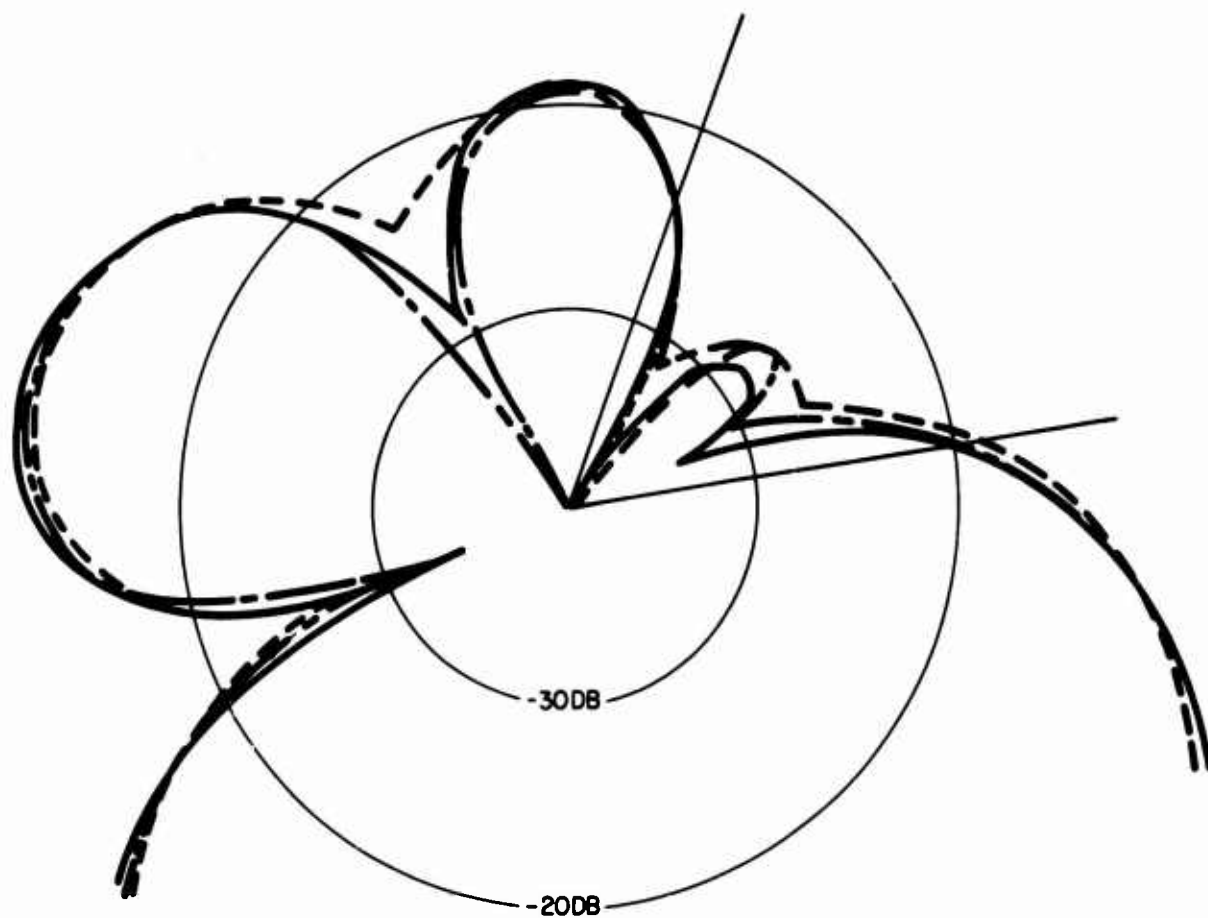


FIGURE 9. Envelope Patterns for Various Loop Separation Distances at 20 kc

$\Delta\alpha = 2^\circ$
 RENULED AT 146°
 --- D=0.7 MI
 — D=1.1 MI
 - - - D=1.5 MI

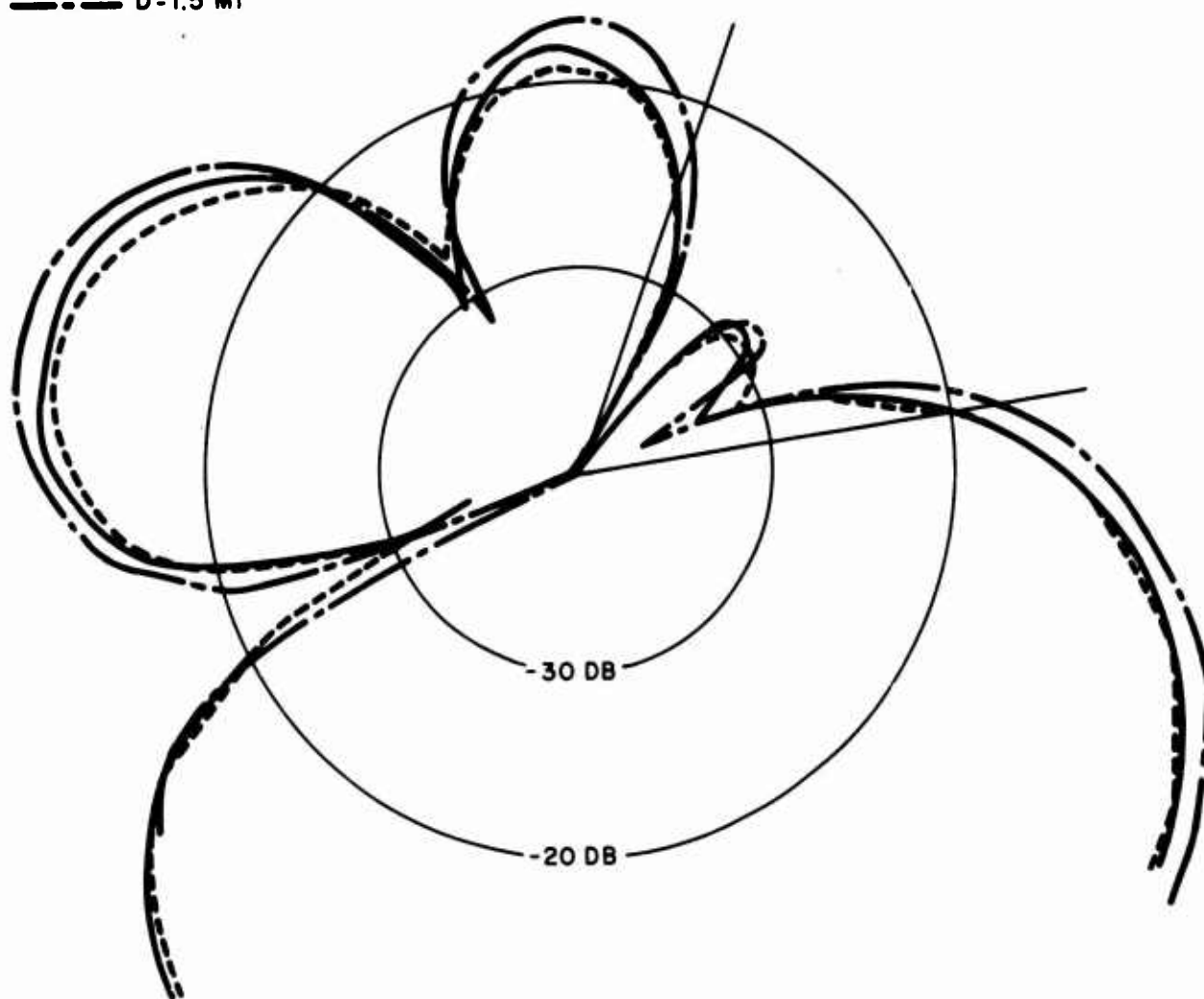


FIGURE 10. Envelope Patterns for Various Loop Separation Distances at 30 kc

of several such relationships have led to the conclusion that a good practical choice for loop separation would be a distance of 1.1 mi. The pattern itself is not highly sensitive to a small variation in this 1.1-mi spacing. It will be noted in these three figures that the 1.5-mi spacing, while providing minor improvement at 10 kc, actually produces pattern degradation at 30 kc relative to the 1.1-mi spacing.

LOOP MISALIGNMENT

The relative angle of each loop axis is quite critical because this produces the deep null at 90° to the plane of the loops. Figure 11 shows how the idealized pattern in Figure 7 would be degraded by 1 and 2° misalignments of the loops with respect to each other. It will be noted in Figure 11 that all of the nulls except the one at 146° are eliminated. Misalignment of the loops would occur during the antenna-construction phase, whereas establishment of a null at 146° is part of the calibration procedure and can be achieved independently of the physical tolerances of the construction process. It is pointed out that a deep null can be achieved at any azimuth in the rear quadrants of the antenna pattern through the adjustment of the amplitude and time-delay values in the summation panel. Where there is a loop misalignment, only one true null can be created in any given pattern. The null most seriously affected is the one at 115° on the idealized pattern (Figure 7). For a 1° loop misalignment (Figure 11) this null degenerates to about -27 db; for a 2° loop misalignment the null is essentially eliminated, the pattern having a value of about -22 db at the 115° angle. This example shows the importance of very careful alignment of the loop elements. Subsequent consideration has led to the conclusion that loop alignment accuracy within 1° can be achieved.

PERFORMANCE CHARACTERISTICS

For evaluation purposes the performance of the superdirective receiving antenna is considered in two categories: (1) assuming that the adjustments were made to obtain a given pattern configuration, what are the effects of the environment, temperature, humidity, and lapsed time on the antenna performance? and (2) assuming that a given pattern can be achieved through adjustments at a given frequency, how well do the components match to maintain this pattern over the desired band of frequencies? In the first case, the pattern variation can be attributed to the performance stability of the components, that is, the preamplifier-gain stability, the stability of the summation panel and transmission line, the time-delay variation in the lumped constant delay line and transmission lines, etc. In the second case, the variables are due to the inability to precisely match components over the full bandwidth; that is, the gain of the two preamplifiers may not be identical over the band. Also, such

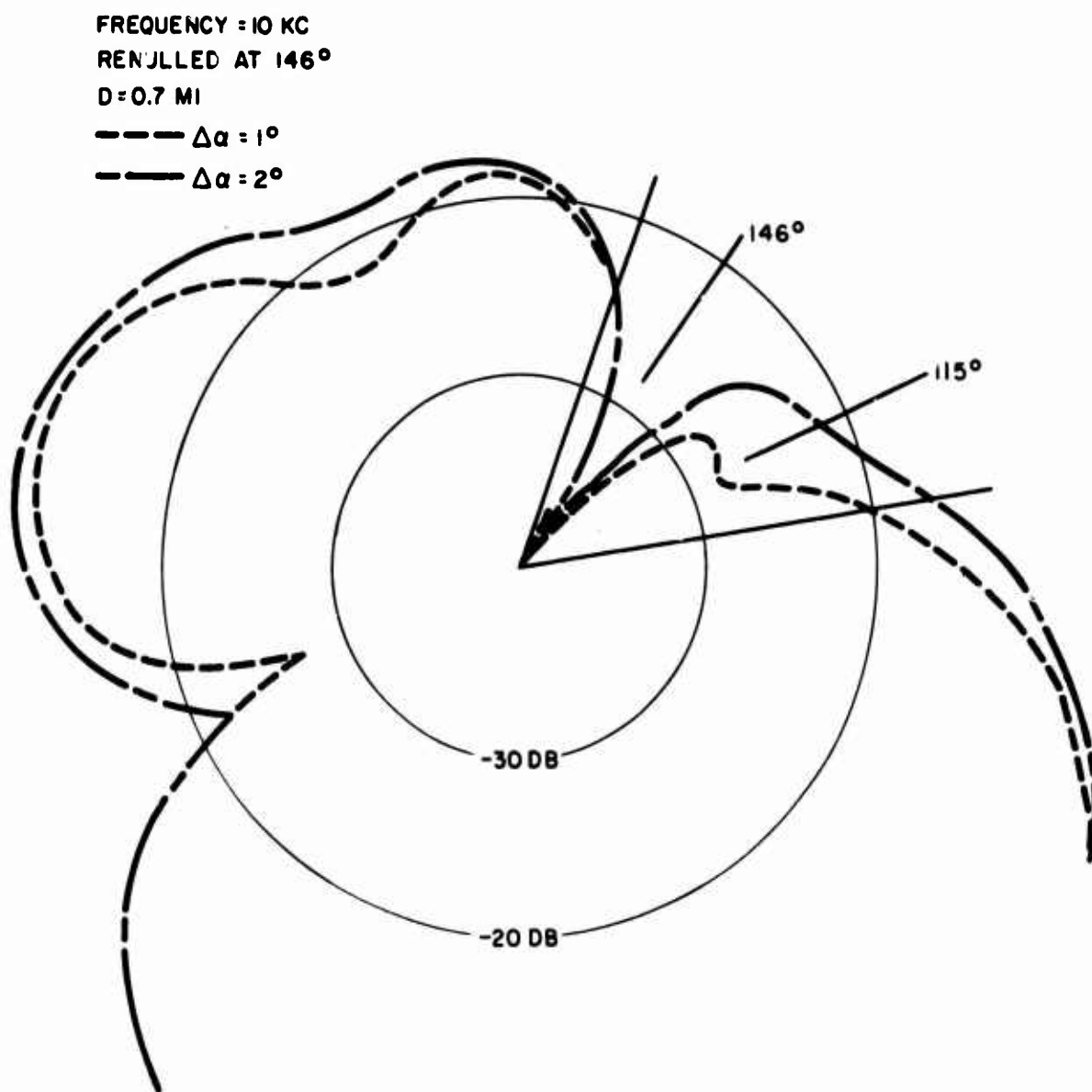


FIGURE 11. Degradation of Idealized Pattern by Misalignment of Loops

items as the matching transformers may have some slight phase shifts which will not be identical as a function of frequency. Under these conditions, even though the proper time delays are obtained for an ideal pattern at one frequency, this pattern will be degraded at other frequencies because of these differences in the component characteristics. In both cases it is the relative characteristics of the components that are important, not their absolute characteristics. For instance, a change in gain-versus-temperature in the preamplifiers is not critical if the behavior of both preamplifiers is identical.

The variables that are considered most important and therefore have been investigated in this study are the relative loop-angle alignment, the relative gain in the two channels from the loops to the summation panel, and the relative time delay between channels. Since all of these are independent variables, a wide combination of possibilities can exist.

Figures 12 through 15 illustrate the changes in minor lobes which result from amplitude differences (ΔA) between the two channels from the loops for different combinations of loop misalignment angle ($\Delta \alpha$) and summation delay error ($\Delta \tau$). The ΔA of 5 percent and the $\Delta \tau$ of 0.5 μ sec are considered extremes and were computed primarily to determine the importance of achieving closer performance tolerances for these parameters. A similar set of curves, Figures 16 through 19, illustrate the changes in pattern that result from time-delay differences between the two loop channels for different combinations of $\Delta \alpha$ and ΔA . Again, it can be seen that the pattern within the 60° sector of prime interest degrades quite rapidly with increasing errors. Yet even in extreme cases the pattern sensitivity is generally 20 db down from the main lobe. In practice it is expected that sufficiently close tolerances can be achieved to maintain a -26 db value within the greatest portion of the 60° sector.

A further comparison to illustrate the magnitude of the pattern degradation between different variables is illustrated in Figure 20, which shows the patterns for a ΔA of 5 percent and for a $\Delta \tau$ of 0.5 μ sec. It can be seen that each of these values produces the same general degradation in pattern, that is, the same general pattern characteristics. The above comparisons are all for 10 kc because given tolerances provide the greatest degradation at this lowest frequency. Also, the atmospheric noise power is greater at this frequency than at the higher frequencies.

A comparison of the degraded patterns for the worst-case conditions, that is, a $\Delta \alpha$ of 1°, a $\Delta \tau$ of 0.5 μ sec, and a ΔA of 5 percent, is shown in Figure 21 for the three frequencies within the band. The poorest pattern is obtained at 10 kc, whereas the 20- and 30-kc patterns show very little difference. As stated earlier, these are envelope patterns, that is, the worst-case condition within the tolerance extremes is plotted for each

FREQUENCY = 10 KC

$\alpha = 25^\circ$

$\phi = 146^\circ$

D = 5000 FT

— $\Delta A = 0$

- - - $\Delta A = 2\%$

- · - $\Delta A = 5\%$

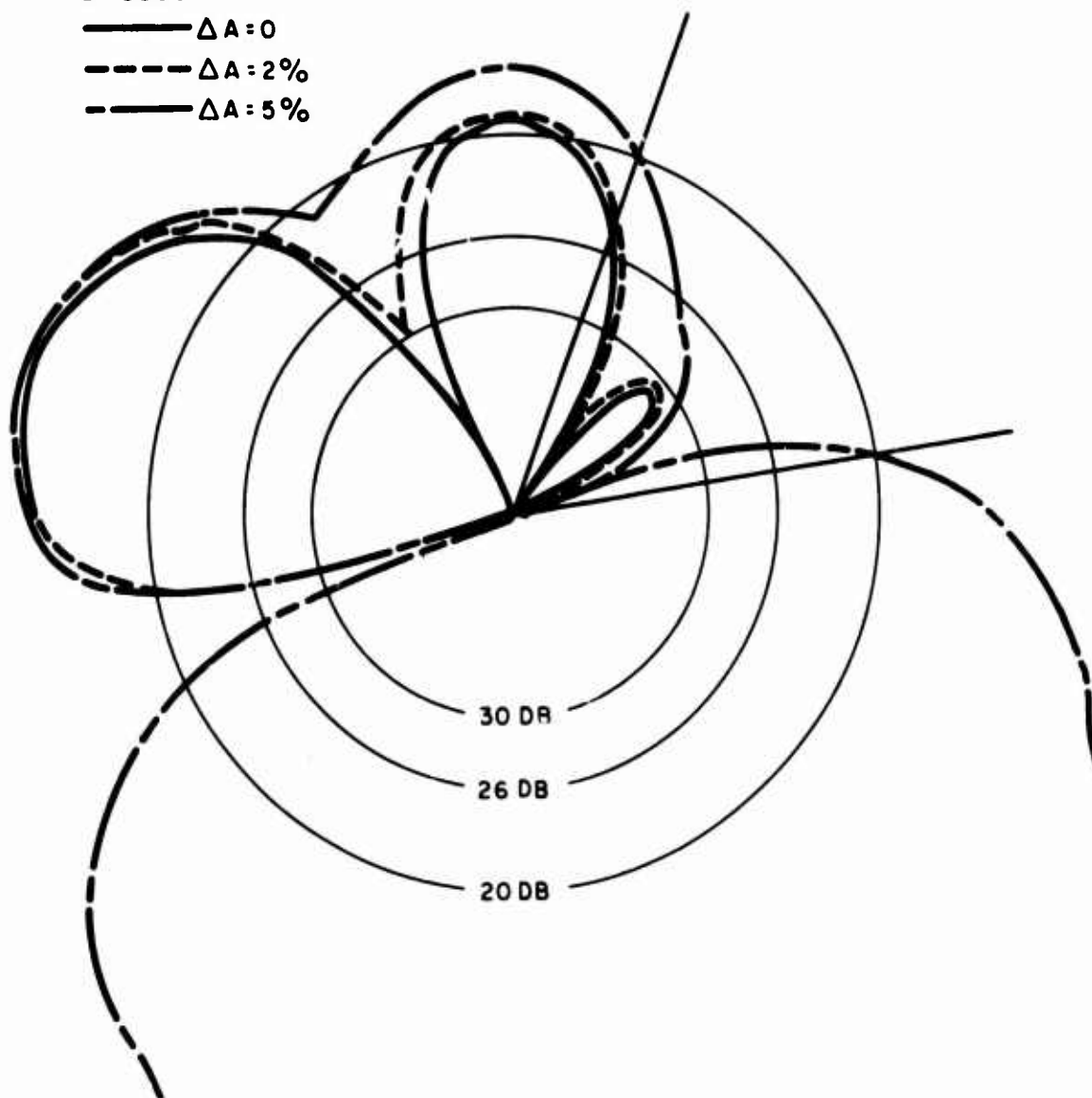


FIGURE 12. Minor-Lobe Changes Caused by Amplitude Differences Between Loop Channels for $\Delta\tau = 0$, $\Delta\alpha = 0$

FREQUENCY = 10 KC

$\alpha = 25^\circ$

$\phi = 146^\circ$

D = 5000 FT

— $\Delta A = 0$

- - $\Delta A = 2\%$

- · - $\Delta A = 5\%$

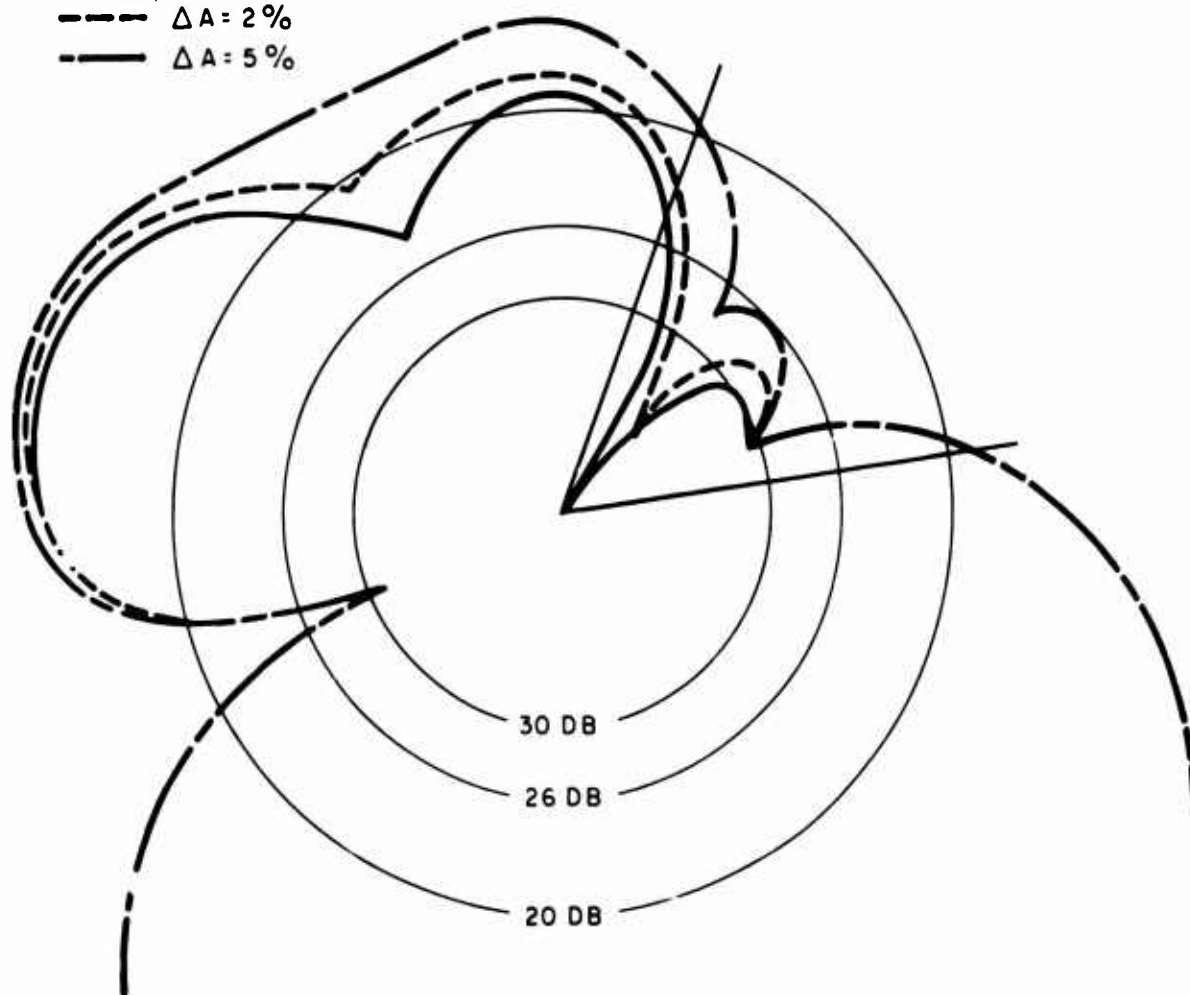


FIGURE 13. Minor-Lobe Changes Caused by Amplitude Differences Between Loop Channels for $\Delta\tau = 0$, $\Delta\alpha = 1^\circ$

FREQUENCY = 10KC

$\alpha = 25^\circ$

$\phi = 146^\circ$

D = 5000 FT

— $\Delta A = 0$

- - - $\Delta A = 2\%$

- · - $\Delta A = 5\%$

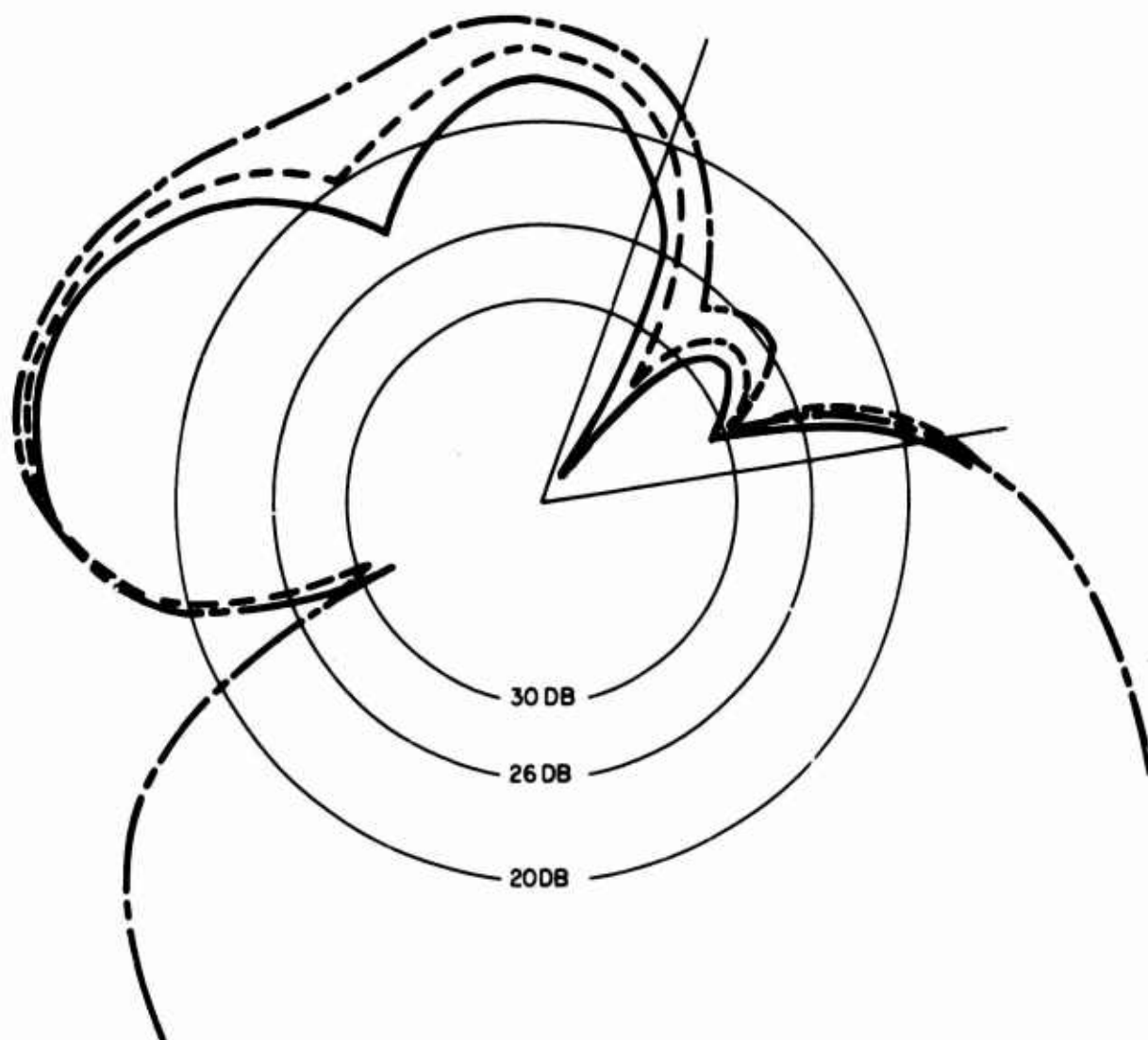


FIGURE 14. Minor-Lobe Changes Caused by Amplitude Differences Between Loop Channels for $\Delta\tau = 0.2 \mu\text{sec}$, $\Delta\alpha = 1^\circ$

FREQUENCY = 10 KC

$\alpha = 25^\circ$

$\phi = 146^\circ$

D = 5000 FT

— $\Delta A = 0$

- - - $\Delta A = 2\%$

- - - $\Delta A = 5\%$

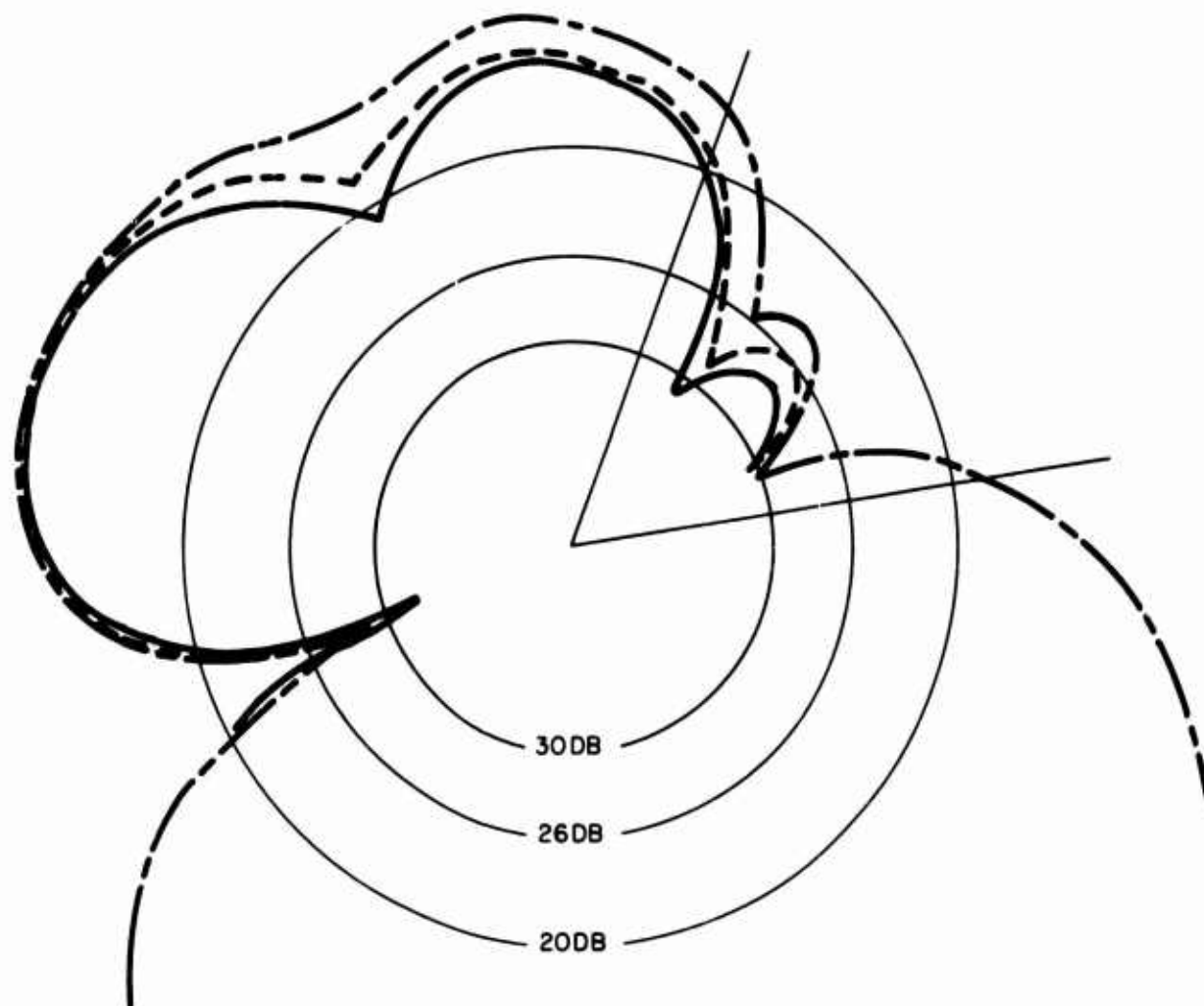


FIGURE 15. Minor-Lobe Changes Caused by Amplitude Differences Between Loop Channels for $\Delta\tau = 0.5 \mu\text{sec}$, $\Delta\alpha = 1^\circ$

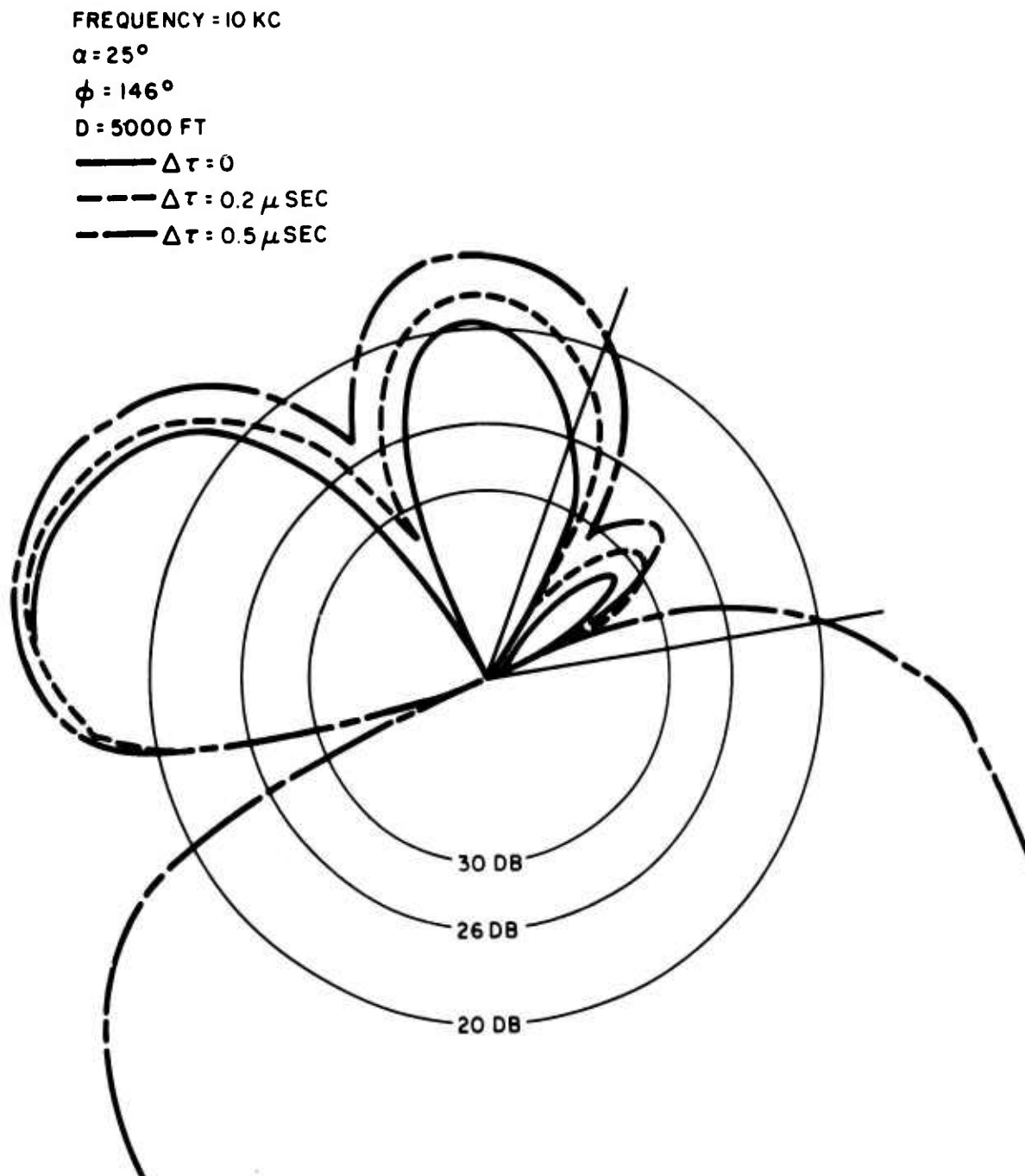


FIGURE 16. Minor-Lobe Changes Caused by Time-Delay Differences Between Loop Channels for $\Delta A = 0$, $\Delta\alpha = 0$

FREQUENCY = 10 KC

$\alpha = 25^\circ$

$\phi = 146^\circ$

D = 5000 FT

— $\Delta\tau = 0$

- - - $\Delta\tau = 0.2 \mu\text{SEC}$

- - - $\Delta\tau = 0.5 \mu\text{SEC}$

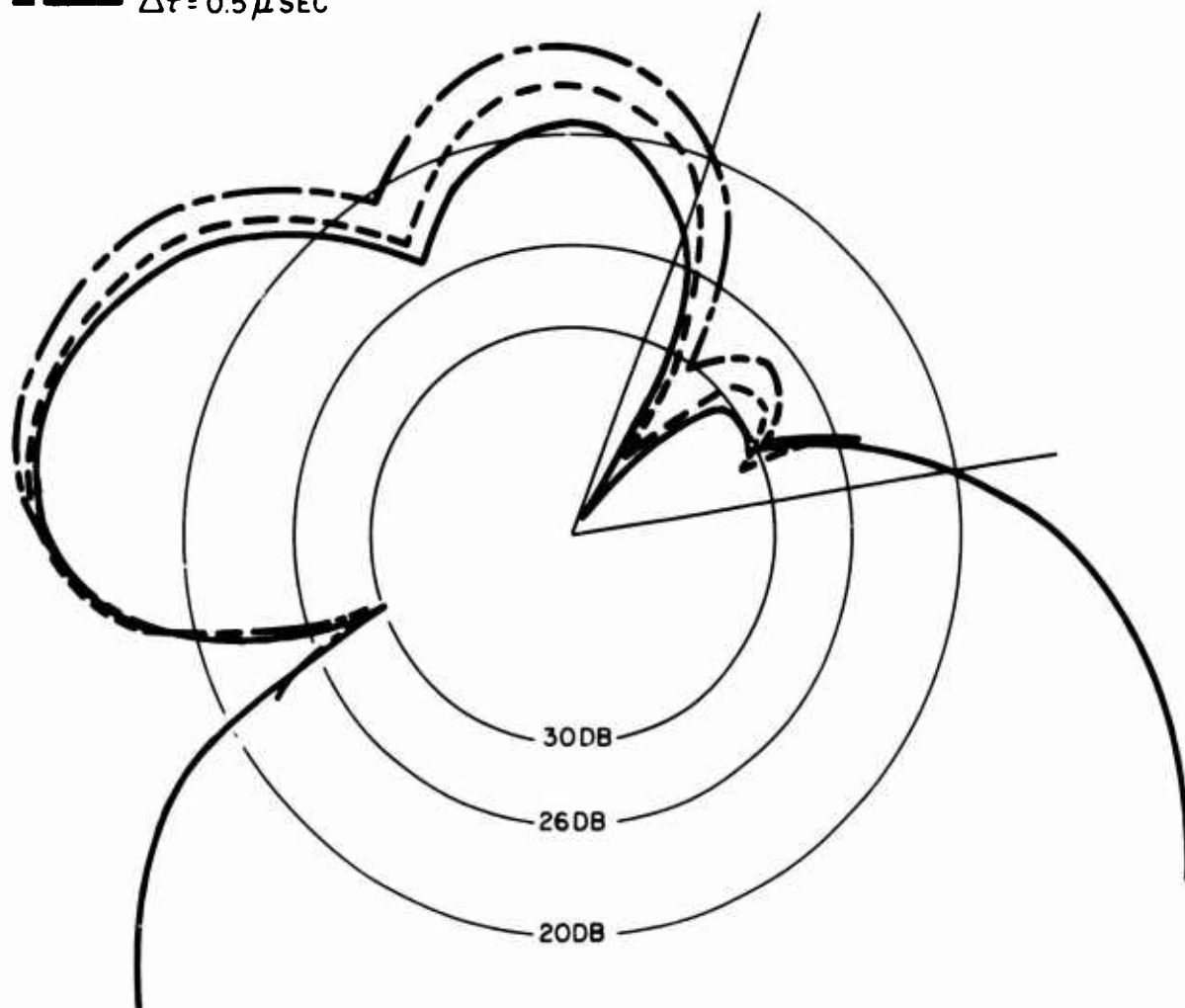


FIGURE 17. Minor-Lobe Changes Caused by Time-Delay Differences Between Loop Channels for $\Delta A = 0$, $\Delta\alpha = 1^\circ$

FREQUENCY = 10 KC

$\alpha = 25^\circ$

$\phi = 146^\circ$

D = 5000 FT

— $\Delta\tau = 0$

- - - $\Delta\tau = 0.2 \mu\text{SEC}$

- · - $\Delta\tau = 0.5 \mu\text{SEC}$

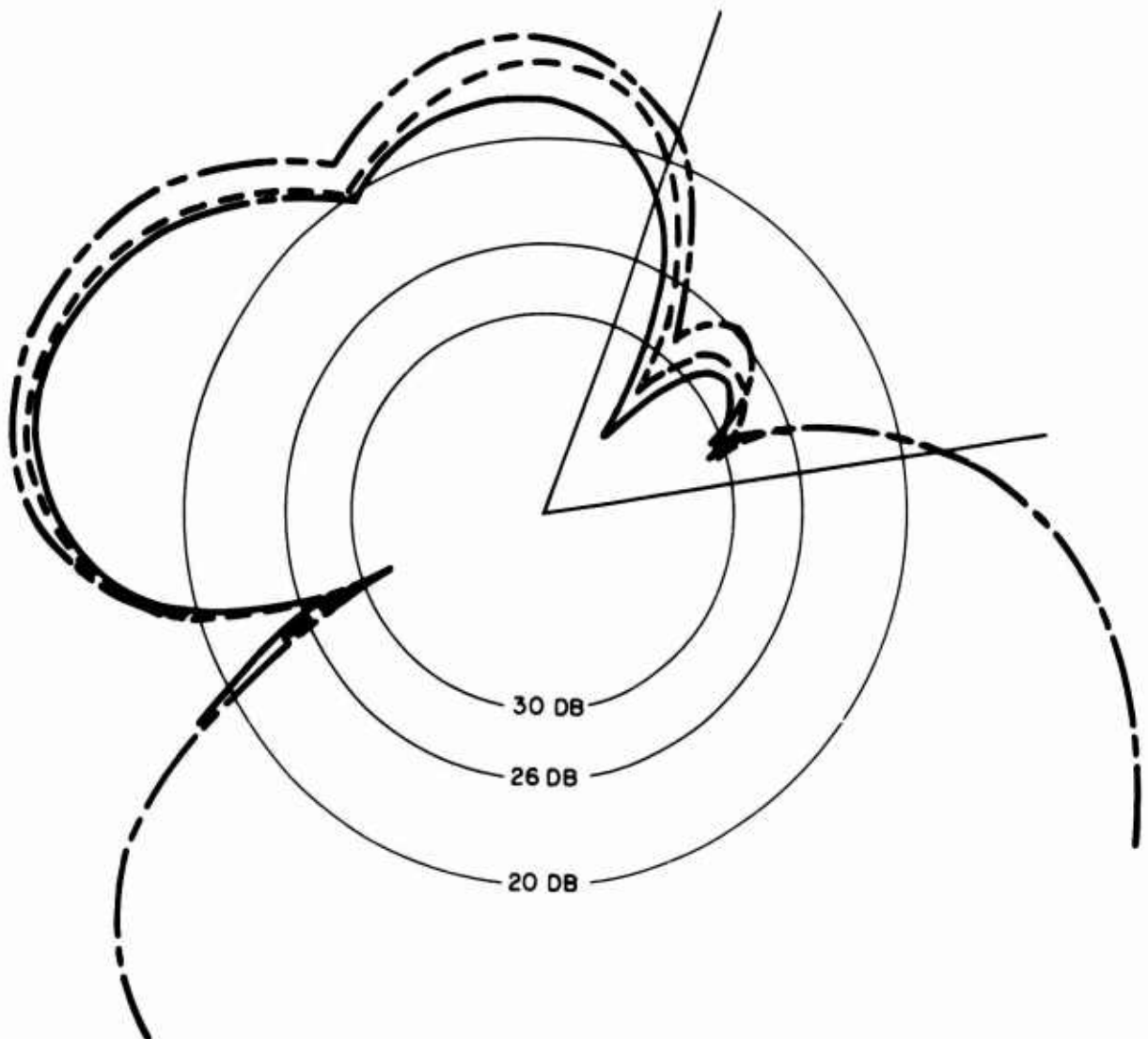


FIGURE 18. Minor-Lobe Changes Caused by Time-Delay Differences Between Loop Channels for $\Delta A = 2\%$, $\Delta\alpha = 1^\circ$

FREQUENCY = 10 KC

$\alpha = 25^\circ$

$\phi = 146^\circ$

D = 5000 FT

— $\Delta\tau = 0$

- - - $\Delta\tau = 0.2 \mu\text{SEC}$

- · - $\Delta\tau = 0.5 \mu\text{SEC}$

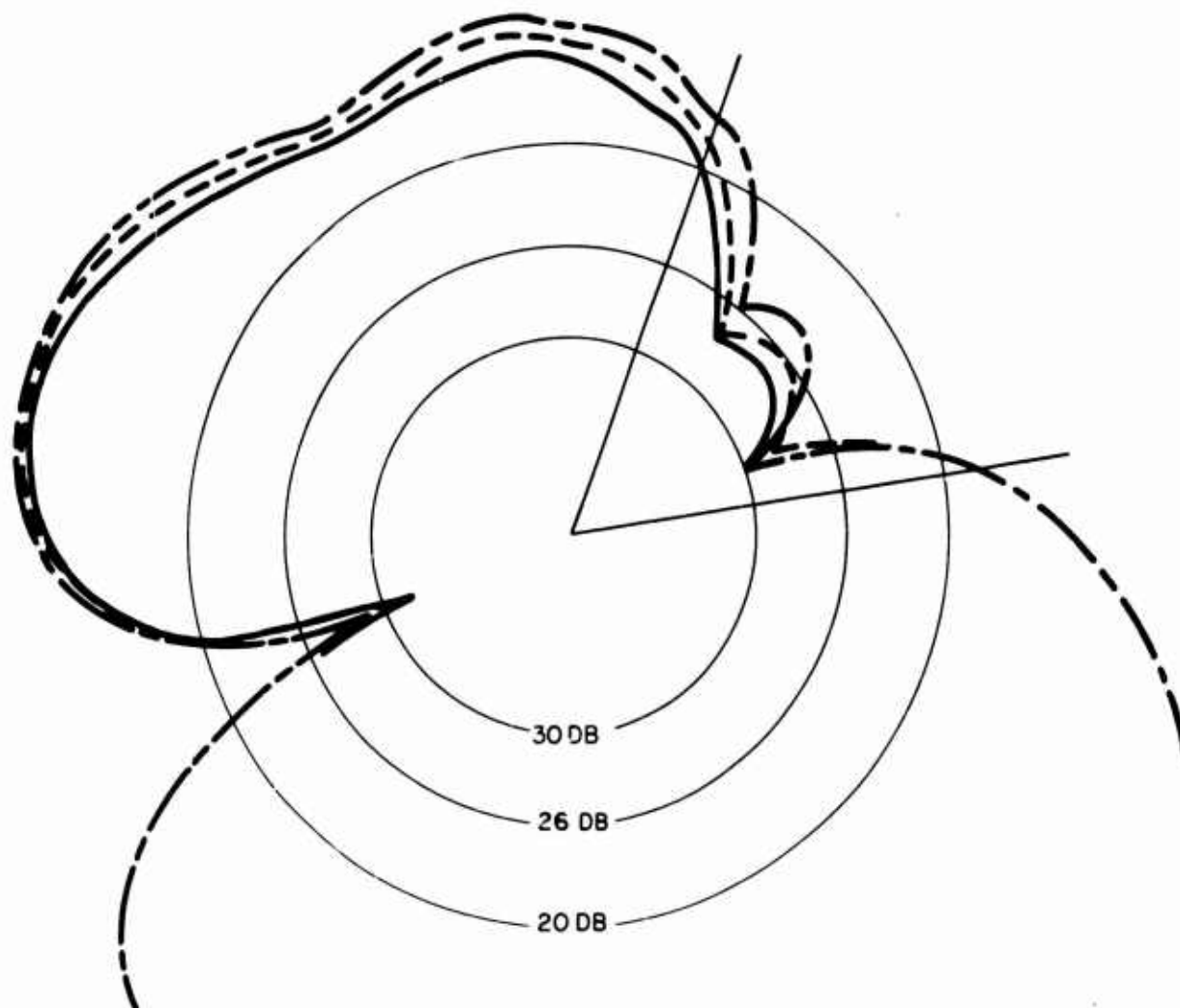


FIGURE 19. Minor-Lobe Changes Caused by Time-Delay Differences Between Loop Channels for $\Delta A = 5\%$, $\Delta\alpha = 1^\circ$

FREQUENCY = 10 KC

$\alpha = 25^\circ$

$\Delta\alpha = 0$

$\phi = 146^\circ$

D = 5000 FT

--- $\Delta\tau = 0.5 \mu\text{SEC}$

— $\Delta A = 5\%$

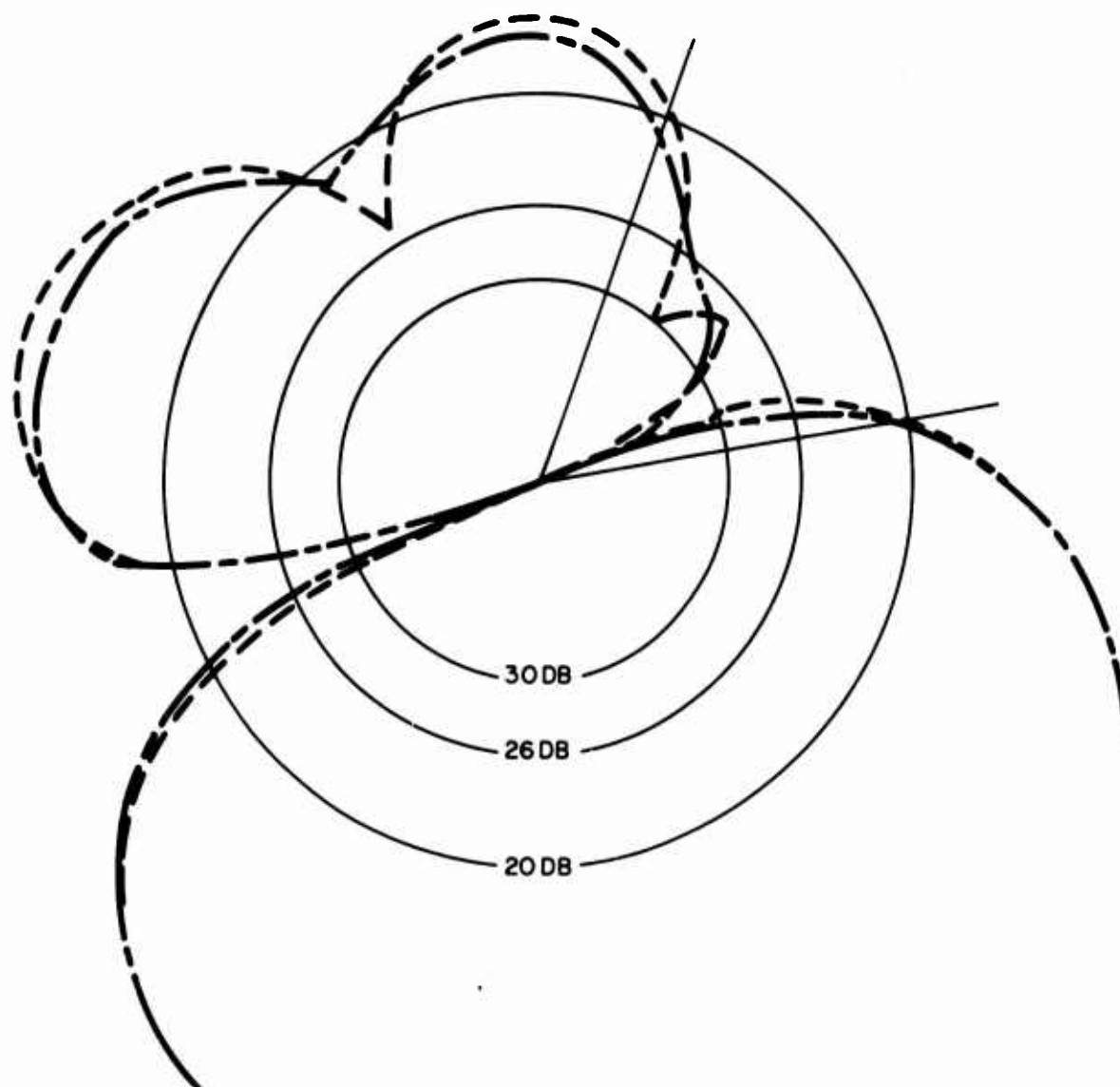


FIGURE 20. Comparison of Minor-Lobe Changes
Caused by ΔA and by $\Delta\tau$

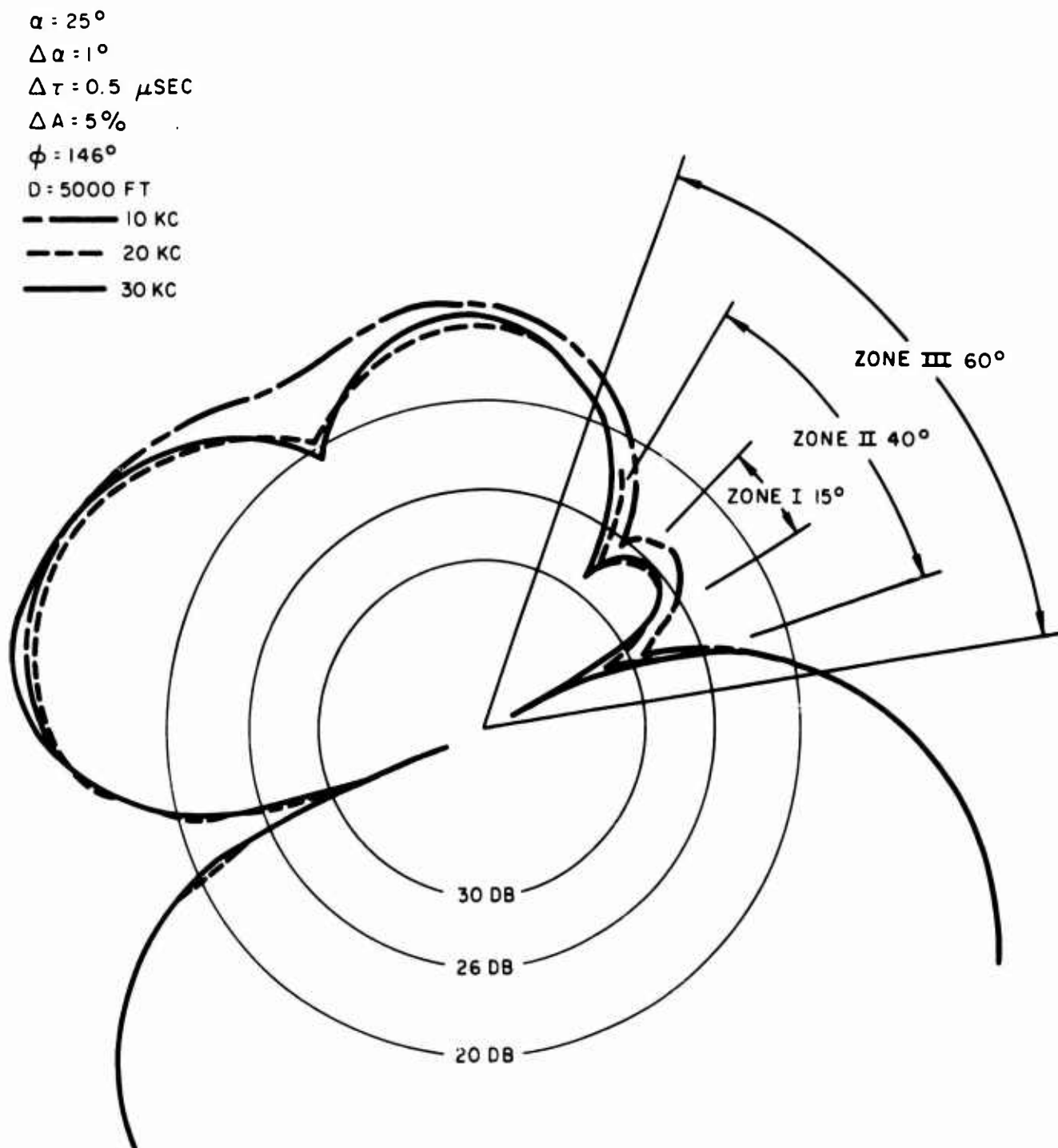


FIGURE 21. Comparison of Minor-Lobe Changes Considering Worst-Case Conditions for Three Frequencies

azimuth. Such patterns are not found in practice; the actual pattern is always somewhat better. For example, Figure 22 illustrates the specific condition where the loop in the direction of the main lobe is rotated 1° clockwise with respect to the plane of the other loop and has an amplitude increased (+) or decreased (-) by 2 percent relative to the other loop. If this loop is rotated 1° counterclockwise with respect to the other loop, the +2 percent and -2 percent ΔA curves will be interchanged from that indicated in this figure.

Finally, it is considered of interest to compare the pattern of one superdirective antenna in which the loops have been rotated 25° from the antenna axis with another in which the loops are parallel to the axis, both for worst-case conditions. The comparison is shown in Figure 23.

PRACTICAL CONSIDERATIONS

The foregoing performance analysis has shown the pattern degradation that is incurred with variations in antenna parameters. This analysis provides the means for specifying tolerance requirements in component design.

It is very important to accurately survey the loop positions during the array construction to make certain that the alignment of the loops is precise. The tolerance in the physical distance between the loops is not stringent. Accuracies of 1° in the relative alignment of loop axes should be readily achievable if the loops are very carefully constructed to be plane. Accuracies within $1/2^\circ$ would be of considerable advantage to the pattern.

Adjustments in the summing panel can be made for precise matching of amplitude from the two channels. However, if the bandpass characteristics of all the components are not identical, this matching can be accomplished over only a limited bandwidth.

From the construction standpoint, the most critical components for achieving a very precise matching of the two channels are the transformers that are used to match the loops to the preamplifiers, the preamplifiers to the transmission lines, and the transmission lines to the summation network. Any slight impedance mismatch at either end of the transformers can create difficulty in achieving identical characteristics over the desired bandwidth. This is particularly true in phase matching, probably more so than in amplitude matching. The transmission line itself can also be a very critical item in that the degree to which propagation characteristics are matched in long transmission lines (approximately 2500 ft) is as yet an unknown parameter.

FREQUENCY = 10 KC

$\alpha = 25^\circ$

$\Delta\alpha = 1^\circ$

$\Delta\tau = 0$

$\phi = 146^\circ$

D = 5000 FT

— $\Delta A = +2\%$ (TRUE PATTERN)

- - - $\Delta A = -2\%$

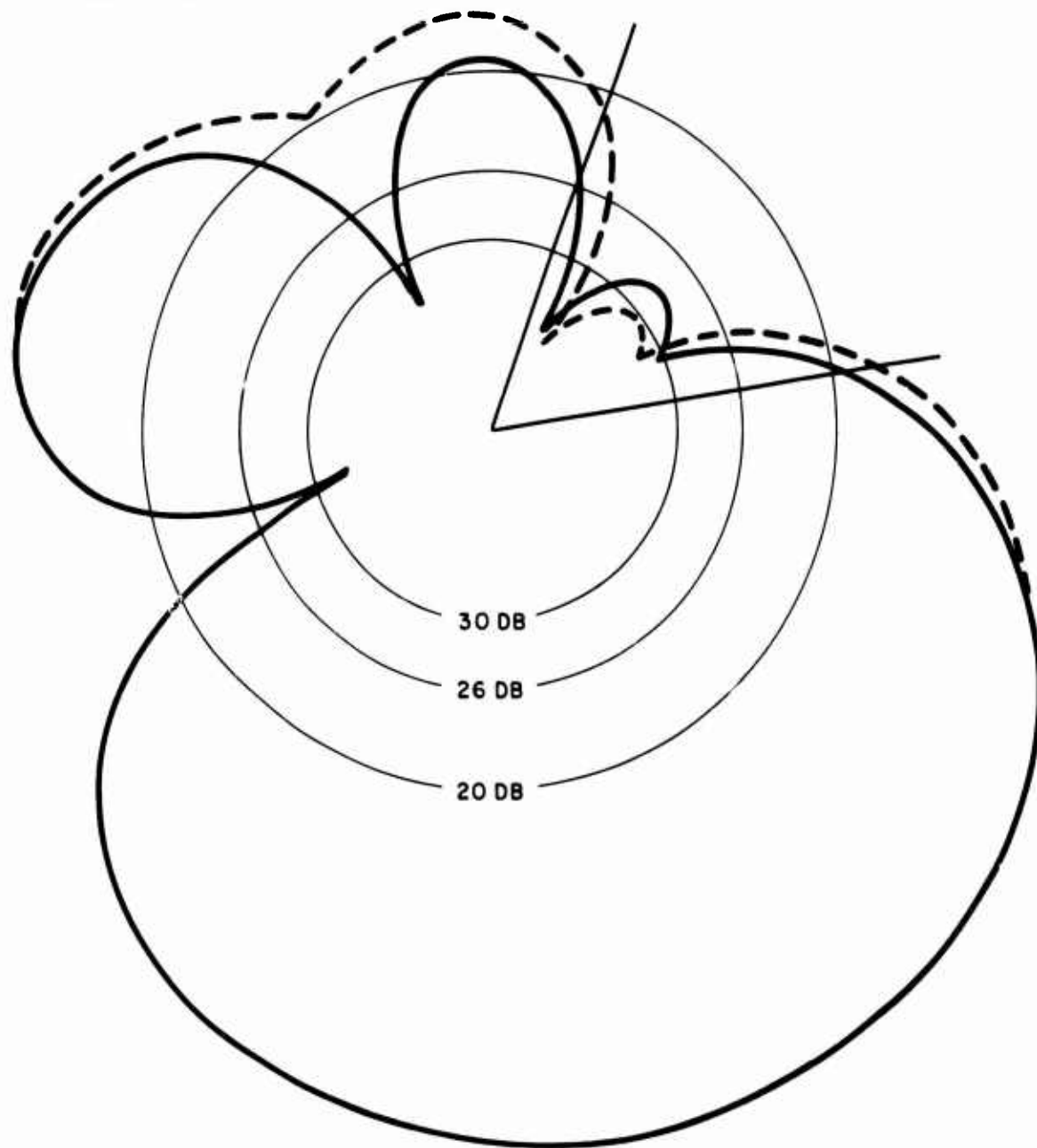


FIGURE 22. Changes in Pattern Where Loop in Direction of Main Lobe Rotated 1° Clockwise With Respect to Other Loop

FREQUENCY = 10 KC

$\Delta \omega = 1^\circ$

$\Delta \tau = 0.5 \mu \text{SEC}$

$\Delta A = 5\%$

$\phi = 146^\circ$

$D = 5000 \text{ FT}$

----- $\alpha = 0$

———— $\alpha = 25^\circ$

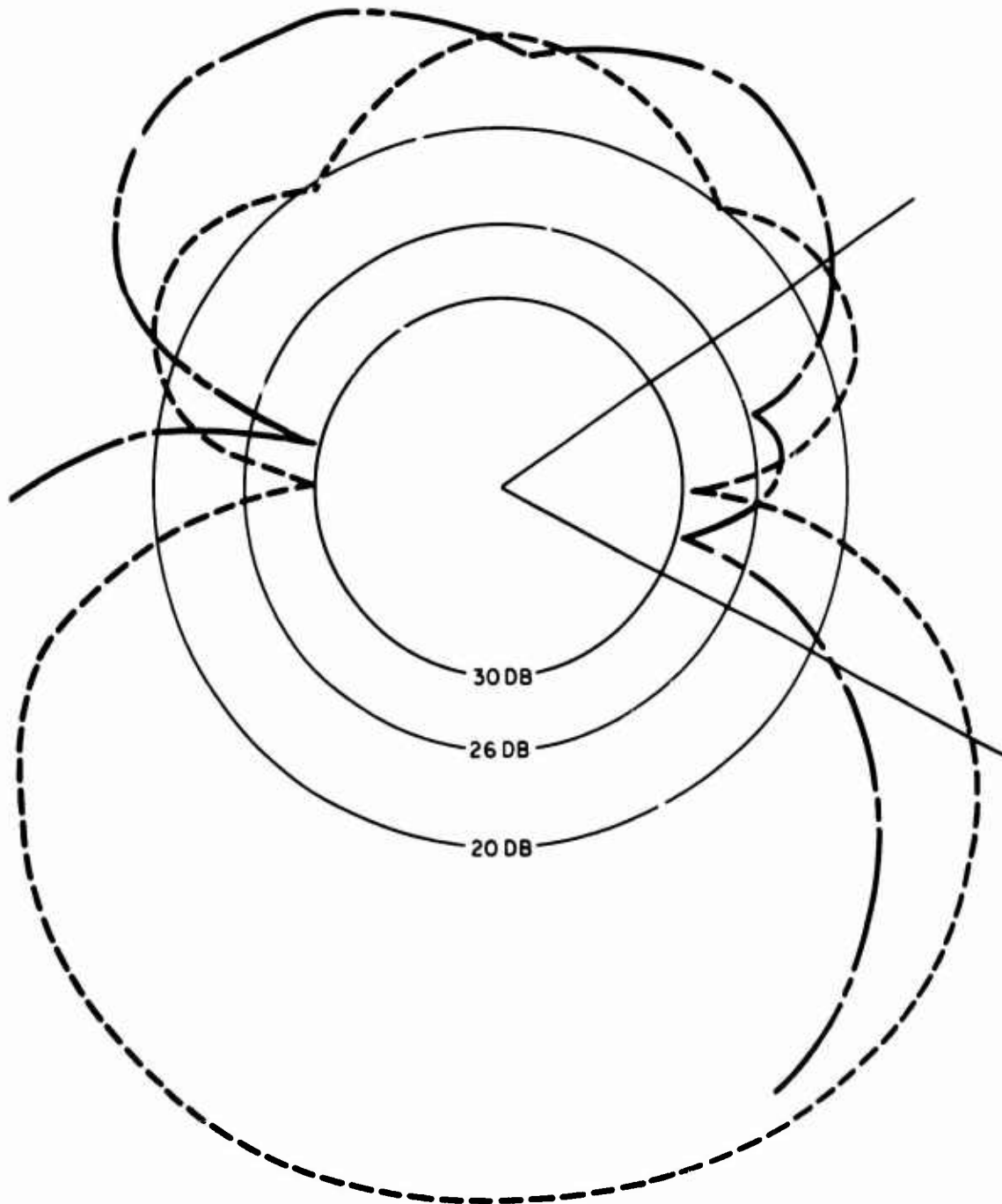


FIGURE 23. Comparison of Antenna Patterns for Different Angles Between Loops and Antenna Axis

For the Bolivian installation, gain and phase stability in the preamplifier along with the matching transformers will be achieved by burying the preamplifiers approximately 2 ft below the surface. Recordings made in the southern California desert over a long period of time have indicated that the temperature variation at this depth can be considerably less than 1°F . It is expected that it will not be practical, however, to bury the transmission lines leading from the loop locations to the receiving site; therefore, a careful examination must be made for any possible variation in propagation loss and in phase in the transmission line caused by large temperature variations.

Finally, improvements in performance over long time periods can be achieved by frequently renulling the antenna to achieve the desired pattern. This operation includes adjustments of the relative amplitude and time delay to maintain the null at the desired location.

Special problems are expected in nulling this antenna in Bolivia in that the only reliable method that has been developed for obtaining a very deep null is to utilize a VLF transmission received from the direction in which the null is to be established. In Bolivia, a transmission is needed from 146° on the pattern, or from a bearing of 28° true. Unfortunately no VLF transmissions are available from that direction. The source closest to that direction is that of GBR at Rugby, England, with transmission at 16 kc arriving from a bearing of 34.3° true. A transmission from an Omega station at Port of Spain, Trinidad, arrives from a bearing of 6.1° true; this station transmits at 10.2 and 13.6 kc. A technique is being developed for nulling on the existing VLF transmission and then steering the null to the desired position by changing the delay-line setting. At the Bolivian site, the null would be obtained on the GBR transmission and then an additional delay of $0.32\ \mu\text{sec}$ would be added to the delay line to steer the null 6° to 146° on the pattern. The problem in this technique is that the additional delay will add more insertion loss in the channel concerned; therefore, amplitude adjustments will be needed to obtain the deep null at the new position. A set of charts will be prepared so that the proper amplitude adjustments can be made along with delay-line adjustments for null rotation.

Checks on the actual pattern achieved can be made by utilizing transmissions from existing VLF transmitters located throughout the world. Figure 24 shows the azimuthal distribution of the VLF transmissions relative to the eclipse path at the Bolivia receiving site.

In conclusion, it has been decided that the utilization of a superdirective antenna with the loops rotated 25° from the antenna axis is a worthwhile undertaking. Even under the most severe performance degradation that could be expected, with this type of antenna, it will provide significant improvements in S/N over that of the simple loop. The experience

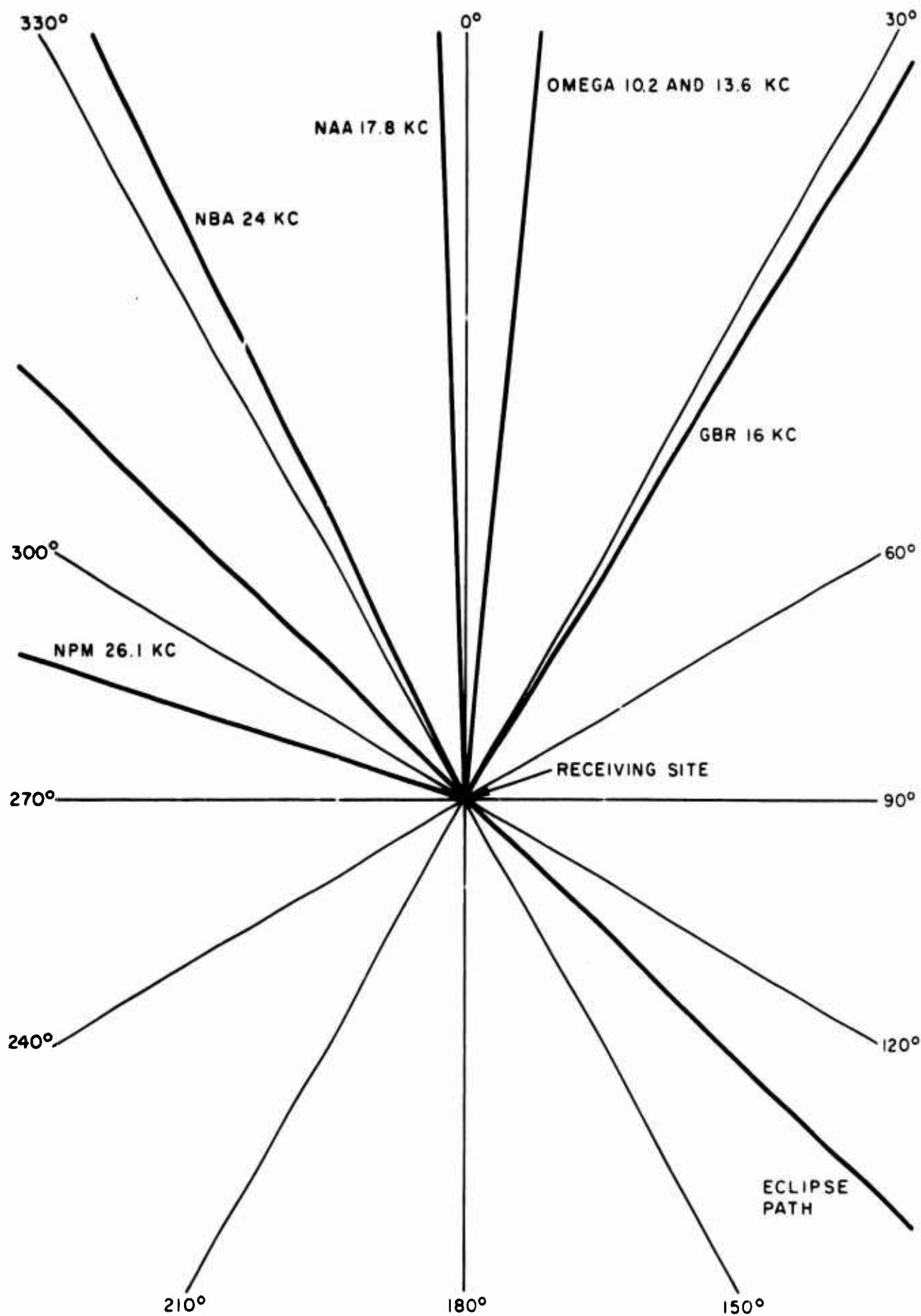


FIGURE 24. Azimuthal Distribution of VLF Transmissions Relative to Eclipse Path for Bolivian Receiving Site

gained in using this antenna configuration will, in itself, be most beneficial. Specific arrangements will be made to evaluate the performance of the antenna and to determine its value in the particular physical situation in Bolivia.

DOCUMENT CONTROL DATA - R & D		
<i>(Security classification of title, body of abstract and indexing annotation must be entered when the overall report is classified)</i>		
1. ORIGINATING ACTIVITY (Corporate author) Naval Ordnance Laboratory Corona, California		2a. REPORT SECURITY CLASSIFICATION UNCLASSIFIED
		2b. GROUP
3. REPORT TITLE SELECTION OF A VLF RECEIVING ANTENNA FOR THE BOLIVIAN SOLAR ECLIPSE SITE		
4. DESCRIPTIVE NOTES (Type of report and inclusive dates) Research report		
5. AUTHOR(S) (First name, middle initial, last name) Hildebrand, Verne E.		
6. REPORT DATE 31 October 1966	7a. TOTAL NO. OF PAGES	7b. NO. OF REFS 3
8a. CONTRACT OR GRANT NO. Defense Atomic Support Agency, REAL,	9a. ORIGINATOR'S REPORT NUMBER(S) NOLC Report 694	
b. PROJECT NO. under MIPER 555-67		
c.	9b. OTHER REPORT NO(S) (Any other numbers that may be assigned this report)	
d.		
10. DISTRIBUTION STATEMENT Distribution of this document is unlimited		
11. SUPPLEMENTARY NOTES	12. SPONSORING MILITARY ACTIVITY Defense Atomic Support Agency	
13. ABSTRACT <p>Properties of the ionosphere D region under conditions of a solar total eclipse are to be measured utilizing a VLF receiving system in Bolivia. The signals will be transmitted from southeast Brazil along the path of totality for the 12 November 1966 solar eclipse.</p> <p>This report describes the study conducted for the selection of a VLF receiving antenna which will provide maximum discrimination against atmospheric noise in the 9- to 31-kc band. The antenna selected was a two-loop superdirective antenna with the loop elements rotated 25° from the antenna axis. The report describes the criteria utilized in selecting the antenna, discusses other possible choices, and evaluates the performance of the antenna in the light of various component tolerances.</p>		

UNCLASSIFIED

14 KEY WORDS	LINK A		LINK B		LINK C	
	ROLE	WT	ROLE	WT	ROLE	WT
Two-loop, superdirective VLF antenna Atmospheric noise discrimination Pattern adjustment Performance analysis Component tolerances						